Multi-bump, self-similar, blow-up solutions of the Ginzburg-Landau equation

Rottschäfer, V.

Available online at www.sciencedirect.com
ScienceDirect
Physica D 237 (2008) 510–539
PHYSICA D
www.elsevier.com/locate/physd

Multi-bump, self-similar, blow-up solutions of the Ginzburg–Landau equation

Vivi Rottschäfer*

Mathematical Institute, Leiden University, P.O. Box 9512, 2300 RA Leiden, The Netherlands
Centre for Mathematics and Computer Science (CWI), P.O. Box 94079, 1090 GB Amsterdam, The Netherlands

Received 8 June 2007; received in revised form 17 September 2007; accepted 23 September 2007
Available online 29 September 2007

Communicated by Y. Nishiura

Abstract

For the Ginzburg–Landau equation (GL), we establish the existence and local uniqueness of two classes of multi-bump, self-similar, blow-up solutions for all dimensions $2 < d < 4$ (under certain conditions on the coefficients in the equation). In numerical simulation and via asymptotic analysis, one class of solutions was already found; the second class of multi-bump solutions is new.

In the analysis, we treat the GL as a small perturbation of the cubic nonlinear Schrödinger equation (NLS). The existence result given here is a major extension of results established previously for the NLS, since for the NLS the construction only holds for d close to the critical dimension $d = 2$.

The behaviour of the self-similar solutions is described by a nonlinear, non-autonomous ordinary differential equation (ODE). After linearisation, this ODE exhibits hyperbolic behaviour near the origin and elliptic behaviour asymptotically. We call the region where the type of behaviour changes the mid-range. All of the bumps of the solutions that we construct lie in the mid-range.

For the construction, we track a manifold of solutions of the ODE that satisfy the condition at the origin forward, and a manifold of solutions that satisfy the asymptotic conditions backward, to a common point in the mid-range. Then, we show that these manifolds intersect transversely. We study the dynamics in the mid-range by using geometric singular perturbation theory, adiabatic Melnikov theory, and the Exchange Lemma.

Keywords: Ginzburg–Landau equation; Multi-bump blow-up solutions

1. Introduction

In various problems coming from physics, biology and chemistry the Ginzburg–Landau equation (GL) is found as a model equation. It is derived in, for example, Rayleigh–Bénard convection, Taylor–Couette flow, nonlinear optics, models of turbulence, superconductivity, superfluidity and reaction–diffusion systems; see [18,3,23,8,9] and the review article [2]. The GL can be viewed as a normal form describing the leading order behaviour of small perturbations in 'marginally unstable' systems of nonlinear partial differential equations defined on unbounded domains [16]. Thus, it is relevant for understanding the dynamics of 'instabilities'. The coefficients in the equation can be expressed in terms of the coefficients of the underlying system of PDEs; therefore, we study the dynamics of the GL for a wide range of parameters.

We study the GL written in the following form:

* Corresponding address: Mathematical Institute, Leiden University, P.O. Box 9512, 2300 RA Leiden, The Netherlands. Tel.: +31 71 52 77 113.
E-mail address: vivi@math.leidenuniv.nl.

0167-2789/$ - see front matter
doi:10.1016/j.physd.2007.09.022

$$\mathrm{i}\frac{\partial \Phi}{\partial t} + (1-\mathrm{i}\varepsilon)\Delta\Phi + (1+\mathrm{i}b\varepsilon)|\Phi|^2\Phi = 0, \tag{1.1}$$

where $x \in \mathbf{R}^d$, $\varepsilon, b > 0$ and $t > 0$. The standard form of the GL as given in [16] can be obtained by rescaling.

Numerical simulations show that there exist sets of initial data for the GL such that the solutions become infinite in finite time for $2 < d < 4$; see [6,19]. Hence, a contraction of the wave packet takes place, and simultaneously the amplitude grows and blows up. In nonlinear optics this phenomenon is called self-focusing and it is related to an extreme increase of the field amplitude. In plasma physics it is called wave collapse.

In this article we study blow-up solutions to the GL as found in the numerical simulations and asymptotic analysis in [6]. We assume $\varepsilon \ll 1$ such that Eq. (1.1) is a small perturbation of the well known nonlinear Schrödinger equation (NLS). Note that, after setting $\varepsilon = 0$ in Eq. (1.1) the GL reduces to the NLS.

Blow-up solutions of the NLS have already been studied extensively; see [24] for a survey. The dimension $d = 2$ is the critical dimension for the NLS; it distinguishes between integrable and blow-up behaviour. In the numerical simulations of [5] and [4], radially symmetric, self-similar, multi-bump blow-up solutions for the NLS were found for $d > 2$. Here, multi-bump is related to $|\Phi|$ having several maxima. An asymptotic analysis was also given in [4]. The existence and local uniqueness of a radially symmetric, monotone, self-similar blow-up solution has been proved for d close to 2 in [15,20]. And the multi-bump solutions have been shown to exist, in [21], again for d close to 2.

Here, we extend and adjust the techniques of [15,20,21] to prove existence and local uniqueness of the blow-up solutions of the GL as found numerically in [6]. The solutions found in [6] are radially symmetric and self-similar as in the case of the NLS. For the NLS, they were studied using the method of dynamical rescaling, and we also use it here. This method exploits the asymptotically self-similar behaviour of the solutions. Following [6], space, time, and Φ are scaled by factors of a suitably chosen norm of the solutions, denoted by $L(t)$, which blows up at the singularity,

$$\xi \equiv \frac{|x|}{L(t)}, \qquad \tau \equiv \int_0^t \frac{1}{L^2(s)}\mathrm{d}s, \qquad u(\xi,\tau) = L(t)\Phi(x,t). \tag{1.2}$$

The corresponding norm of the rescaled solution u remains constant in time, and as a consequence, the rescaled problem is no longer singular. The rescaled solution u satisfies

$$\mathrm{i}u_\tau + (1-\mathrm{i}\varepsilon)\left[u_{\xi\xi} + \frac{d-1}{\xi}u_\xi\right] + (1+\mathrm{i}b\varepsilon)|u|^2u + \mathrm{i}a(\tau)(\xi u)_\xi = 0,$$

where

$$a = -L\frac{\mathrm{d}L}{\mathrm{d}t} = -\frac{1}{L}\frac{\mathrm{d}L}{\mathrm{d}\tau}.$$

Self-similar blow-up behaviour, with $L(t) \to 0$, arises when $a(\tau)$ is a positive constant and $u(\xi,\tau) = \mathrm{e}^{\mathrm{i}w\tau}Q(\xi)$ for some positive w that depends on the solution. We have $L(t) = \sqrt{2a(T-t)}$ and $\tau = \frac{1}{2a}\log(T-t)$, and scaling τ with $\frac{1}{w}$ leads to the following equation for Q:

$$(1-\mathrm{i}\varepsilon)\left[Q_{\xi\xi} + \frac{(d-1)}{\xi}Q_\xi\right] - Q + \mathrm{i}a(\xi Q)_\xi + (1+\mathrm{i}b\varepsilon)|Q|^2Q = 0. \tag{1.3}$$

Here the parameter a plays the role of a nonlinear eigenvalue. In [19], the constant w is left as an unknown; this does not affect the solutions since it can be scaled out.

Moreover, the initial and asymptotic conditions for Φ, namely that $\Phi(x,0) = \Phi_0(x)$ and that $|\Phi|$ vanishes as $|x| \to \infty$, lead to the following initial and asymptotic conditions for Q:

$$Q_\xi(0) = 0, \quad \operatorname{Im} Q(0) = 0, \tag{1.4}$$

$$|Q(\xi)| \to 0 \quad \text{as } \xi \to \infty. \tag{1.5}$$

Here we have exploited the phase invariance of the equation to define the phase of Φ at the origin. Alternatively, we could have kept w as an unknown in (1.3) and set $Q(0) = 1$, as in [19].

In the numerics and asymptotics in [6], multi-bump solutions were found where $|Q|$ has k maxima on the real line. For every $2 < d < 4$, k-solution branches are found in the (ε, a)-plane on which a solution with k maxima on $(-\infty, \infty)$ exists. In Fig. 1(a), which is a reproduction of Fig. 1.1 from [6], the branches for $k = 1$ and $k = 2$ where $b = 0$ and $d = 3$ are given. The branches correspond to symmetric solutions with one maximum on the real line, $k = 1$, at $\xi = 0$, and with two maxima, $k = 2$, on the real line. The latter solutions ($k = 2$) have a minimum at $\xi = 0$. The amplitudes $|Q|$ of the solutions as found on the upper and lower parts of both branches at $\varepsilon = 0.1$, the points indicated by the *'s, are given in Fig. 1(b), which is a reproduction of Fig. 1.2 from [6].

Every k-solution branch consists of two parts which coalesce. The solutions on the upper part of the branch are smooth perturbations of the solutions found for the NLS. Note that the intersection point of this part of the branch with the $\varepsilon = 0$-axis

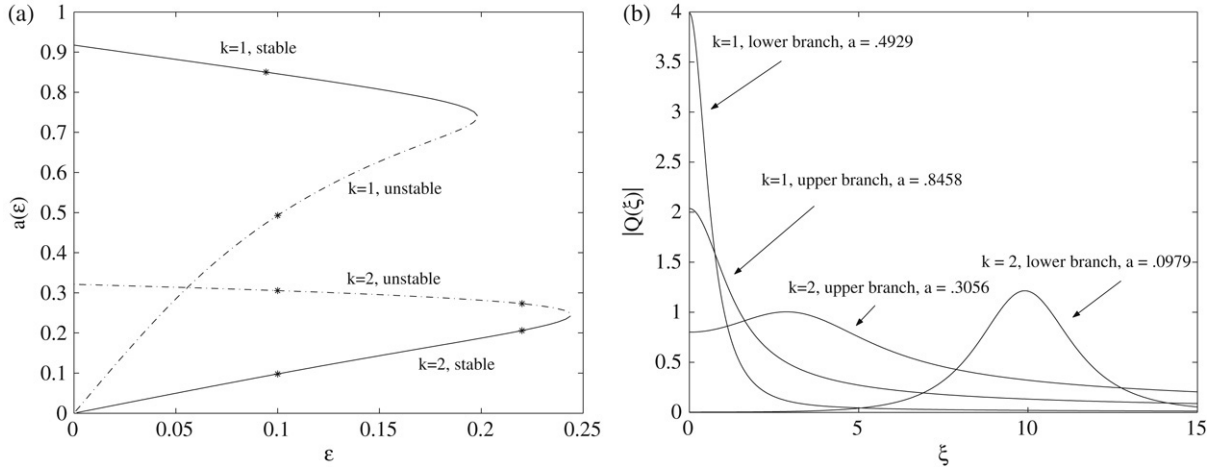

Fig. 1. (a) The $k = 1$ solution branch, the solutions with one maximum on $(-\infty, \infty)$, and the $k = 2$ solution branch, the solutions with two maxima on $(-\infty, \infty)$, plotted in the (ε, a)-plane where $d = 3$ and $b = 0$. In (b), the solutions corresponding to the *'s are given. (b) Final-time profiles where the amplitude $|Q|$ is plotted as a function of the spatial variable ξ for $\varepsilon = 0.1$. The solutions correspond to the *'s in (a). This is a reproduction of Figs. 1.1 and 1.2 in [6].

corresponds exactly to the NLS solutions. However, solutions on the lower part of the branch are not a simple perturbation of the solutions of the NLS.

There is a clear distinction between solutions for which k is even and ones for which it is odd. When k is odd the k-solution has a maximum at $\xi = 0$; on the other hand for even k it does not.

In the numerical simulations, the maxima that lie away from $\xi = 0$ are found for a small in the range $\xi = \mathcal{O}(\frac{1}{a})$ and just to the left of $\xi = \frac{2}{a}$, which is the point where the linearisation of (1.3) has a turning point. Thus, as $a \to 0^+$, all these maxima are created at $|\xi| = \infty$. Furthermore, for k odd and $d \to 2^+$ the form of $|Q|$ close to $\xi = 0$ converges to the ground state solution of

$$R_{\xi\xi} + \frac{d-1}{\xi} R_\xi - R + R^3 = 0. \tag{1.6}$$

In this article, we focus mainly on the solutions as found on the lower part of the k-solution branches. More specifically, we construct the solutions for k even; the solutions with a minimum at $\xi = 0$. This is one of the main points in which the analysis of this article differs from and extends the studies in [21,20,15] (apart from the fact that the equation is different). There, solutions with a maximum at $\xi = 0$ were constructed for the NLS. So far, no analysis for the solutions with a minimum at $\xi = 0$ has been performed.

For k even, we establish existence and local uniqueness of two classes of k-bump solutions for $2 < d < 4$ and with $0 < a \ll 1$ as long as certain relations between a, d, b and ε hold. The second major extension of [21,20,15] is the fact that our proof holds for every $2 < d < 4$, whereas in the studies for the NLS [20,21] the dimension d must be taken algebraically close to $d = 2$: $d - 2 = \mathcal{O}(a^l)$ for some $l > 0$. This extended result is possible because we focus mainly on solutions on the lower part of the solution branches. These solutions are no simple perturbations of the solutions for the NLS. Nevertheless, for d algebraically close to 2 the analysis here also yields the solutions on the upper part of the branches.

In the analysis, we find that the $\frac{k}{2}$ maxima for $\xi > 0$ (recall that the solution is symmetric) lie just to the left of $\xi = \frac{2}{a}$ and are $\mathcal{O}(\log \frac{1}{a})$ apart. These maxima lie in the so-called mid-range, the interval $\xi \in [\xi_b, \xi_{\max}]$ where $\xi_b = k_b \log \frac{1}{a}$ and $\xi_{\max} = \frac{2-\sqrt{a}}{a}$. The two types of solutions that are constructed differ from one another in the value of $|Q|$ at $\xi = \xi_{\max}$. For solutions of type L, $|Q|$ is exponentially small at $\xi = \xi_{\max}$ whereas for solutions of type R, $|Q|(\xi_{\max})$ is strictly $\mathcal{O}(a^{\frac{3}{8}})$. The solutions of type L are those found in [6]. The solutions of type R have, to our knowledge, not been found in numerical simulations or asymptotic analysis so far. Finally, the solutions of type L lie exponentially close to each other as do the solutions of type R.

Solutions with a maximum at $\xi = 0$, where k is odd, can also be found for the GL by combining the techniques from this article and Section 4 of [21]. We do not give a proof here, but we will state the results in the next section.

Remark 1.1. Choosing a non-integer dimension as done here is equivalent to taking $d = 2$ and the power of the nonlinear term equal to 2σ for some positive σ.

2. The main result and the strategy for its proof

In this section, we state the main theorem and the strategy that we take to prove it. The main result of this paper is

Theorem 2.1. *For each $a > 0$ sufficiently small, $2 < d < 4$, and d, ε, b and a related as in expressions (2.1) and (2.2), there exists an $n_0(a)$ such that, if $2 \leq n \leq n_0(a)$ and n is even, there exist $2n$ locally unique $k = n$ solutions of the type studied here of the problem given by Eq. (1.3) and the initial conditions (1.4) and boundary conditions (1.5). These symmetric solutions consist of n maxima on the real line where $\frac{n}{2}$ maxima are found on $0 < \xi < \xi_{\max}$, with $\xi_{\max} = \frac{2-\sqrt{a}}{a}$. These maxima are strictly $\mathcal{O}(\log(\frac{1}{a}))$ apart. Of the $2n$ locally unique $k = n$ solutions, $n+1$ are characterized by the property that $|Q(\xi_{\max})|$ is exponentially small, and they are said to be of type L. The other $n-1$, said to be of type R, instead satisfy $|Q(\xi_{\max})| = ca^{3/8} - \tilde{c}a^{5/8}$, for some positive constant c and a positive function $\tilde{c} = \tilde{c}(c)$, and the last maximum occurs near $\xi_{\max}$, where $|Q| = \sqrt{2}a^{\frac{1}{4}}(1 - \frac{1}{8}\sqrt{a}) + hot$.*

We now give the restrictions under which this theorem holds. First of all, we aim for a balance in Eq. (1.3) between the terms containing the parameter ε, representing the perturbation away from the NLS giving the GL, and the terms containing the small parameter a, and therefore, set

$$\varepsilon = Ka, \tag{2.1}$$

where $K > 0$ and $K = \mathcal{O}(1)$.

Moreover, we assume when bounding ϕ in Section 7 that there exist constants $c_1, c_2, c, \tilde{c} > 0$, c_3 and $l > \frac{1}{2}$ such that d, ε, b and a satisfy

$$|c_1 a(d-2) - c_2\varepsilon + c_3 ab| \leq ca^{\frac{1}{4}+l}\mathrm{e}^{-\frac{\tilde{c}}{a}}. \tag{2.2}$$

For every solution, the constants c_i can be determined; they differ as k is varied. Moreover, restriction (2.2) can be made less strict (replacing the exponentially small term by a term of $\mathcal{O}(a^{l_1})$), yielding fewer solutions in the theorem; see Remark 7.1. It is remarkable that in this case, for every even k a k-solution can still be constructed.

Note that it is possible to choose a, d, ε and b in such a way that restriction (2.2) is satisfied. For example, if we focus on the two-bump solutions in the case where $b = 0$, relation (2.2) reduces to

$$\left|\frac{d-2}{2} - \frac{5}{3}K\right| + \frac{8\sqrt{2}}{9\sqrt{3}}K \leq ca^{-\frac{3}{4}+l}\mathrm{e}^{-\frac{\tilde{c}}{a}}; \tag{2.3}$$

see Lemma 7.2 and expression (7.3). And ε, a and d can indeed be chosen such that this holds.

Remark 2.1. It will be shown that $n_0(a)$ increases as a decreases.

For solutions with a maximum at the origin, and hence, an odd number of maxima (n odd), a statement similar to Theorem 2.1 can be proved. The result and assumptions only slightly change. Combination of the proofs given in this article and in Section 4 of [21] leads to the existence of $4(n-1)$ locally unique n-solutions for n odd. Moreover, the two different types of solutions in the theorem still exist and they are characterised by the same properties. There exist $2n-1$ solutions of type L and the other $2n-3$ are of type R. Assumption (2.1) still has to be satisfied whereas restriction (2.2) must be replaced by

$$|\tilde{c}_1 a(d-2) - \tilde{c}_2\varepsilon + \tilde{c}_3 ab| \leq \hat{c}a^{\frac{5}{4}+l}, \tag{2.4}$$

leading to a less strict condition on a, d, ε and b.

We study solutions of Eq. (1.3) with initial condition (1.4) and boundary condition (1.5). As in [6] and the studies for the NLS [21,20,15], we replace the boundary condition (1.5) by a local asymptotic condition at $\xi \to \infty$. For large ξ, it follows from the boundary condition (1.5), $|Q(\xi)| \to 0$, that the behaviour of the solutions is described by the linear part of Eq. (1.3):

$$(1 - \mathrm{i}aK)\left[Q_{\xi\xi} + \frac{(d-1)}{\xi}Q_\xi\right] - Q + \mathrm{i}a(\xi Q)_\xi = 0. \tag{2.5}$$

For this equation, there exists a pair of linearly independent solutions for large ξ that are given by

$$Q_1 \sim \xi^{-1-\frac{\mathrm{i}}{a}}, \qquad Q_2 \sim \xi^{-(d-1-\frac{\mathrm{i}}{a})}\mathrm{e}^{-\mathrm{i}a\frac{\xi^2}{2} + \frac{a^2K\xi^2}{2}}. \tag{2.6}$$

Solution Q_2 is rapidly varying as $|\xi| \to \infty$, and has unbounded H^1-norm. The solutions that we are looking for are slowly varying solutions, and hence, their limiting profile for large ξ is a multiple of Q_1. The asymptotic expressions for Q_1 and its derivative imply that

$$\left|\xi Q_\xi + \left(1 + \frac{\mathrm{i}}{a}\right)Q\right| \to 0 \quad \text{as } \xi \to \infty \tag{2.7}$$

must hold; see [6]. In the NLS limit this corresponds to solutions with finite Hamiltonian. From the fact that Q_1 decays at ∞, it follows that the boundary condition (1.5) is satisfied, and hence, condition (1.5) can be omitted. Therefore, we from now on study Eq. (1.3) with the conditions (1.4) and (2.7).

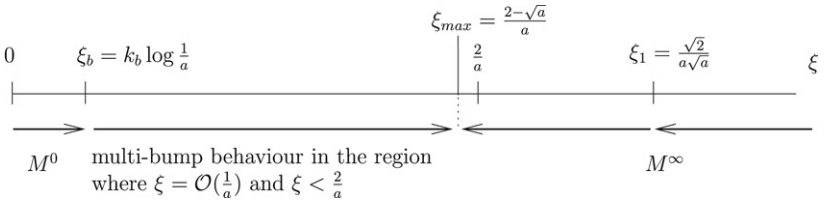

Fig. 2. The different points and intervals on the ξ-axis. As explained in Section 2, solutions on the manifolds M^∞ and M^0 are tracked to $\xi_{\max}$ from ∞ and 0, respectively, and it is shown that these manifolds have two families of transverse intersection points at $\xi_{\max}$. The multi-bump, self-similar, blow-up solutions of Theorem 2.1 are found in these transverse intersections.

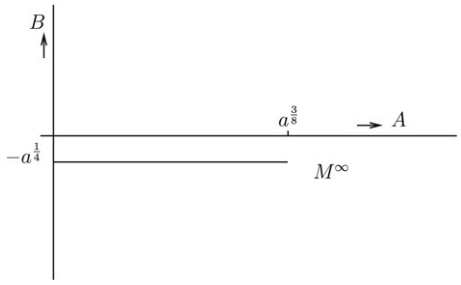

Fig. 3. A sketch of the manifold M^∞ in the A–B plane at $\xi = \xi_{\max}$.

The analysis of (1.3) is carried out by decomposing Q into amplitude and phase,

$$Q(\xi) = A(\xi) \exp\left[\mathrm{i} \int_0^\xi \psi(x)\mathrm{d}x\right], \qquad B(\xi) = \frac{A_\xi}{A}. \tag{2.8}$$

Here, A is the amplitude, B its logarithmic derivative, and ψ is the gradient of the phase. Then, (1.3) reduces to

$$\begin{cases} A_\xi = AB \\ B_\xi = \dfrac{(1-d)B}{\xi} + \psi^2 - B^2 + \dfrac{1}{1+a^2K^2}[-(1-a^2bK^2)A^2 + 1 + a\xi\psi + a^2K(1+\xi B)] \\ \psi_\xi = \dfrac{(1-d)\psi}{\xi} - 2\psi B - \dfrac{a}{1+a^2K^2}[1 + \xi B + K((1+b)A^2 - 1 - a\xi\psi)], \end{cases} \tag{2.9}$$

where (1.4) and (2.7) are given by

$$B(0) = 0, \qquad \psi(0) = 0, \tag{2.10}$$

and

$$B \sim -\frac{1}{\xi}, \qquad \psi \sim -\frac{1}{a\xi} \quad \text{as } \xi \to \infty. \tag{2.11}$$

This reduction from a four-dimensional system to a three-dimensional system is made possible by the fact that Eq. (1.3) is invariant under phase shifts.

We prove Theorem 2.1 by analysing the solutions of Eq. (2.9) that satisfy the initial and asymptotic conditions (2.10) and (2.11). We start with those solutions that satisfy (2.11). These form a three-dimensional manifold in the A–B–ψ–ξ–d extended phase space, and we denote this manifold by M^∞, where the superscript ∞ corresponds to the fact that they satisfy (2.11); the condition at infinity. By tracking these solutions from ∞ back to $\xi = \xi_{\max} = \frac{2-\sqrt{a}}{a}$ (see Fig. 2), we find that, at $\xi_{\max}$, a segment of the manifold M^∞ is nearly a horizontal line segment that stretches out at least over the interval $(0, a^{3/8}]$ in the A coordinate with $B = -a^{1/4}$ to leading order; see Fig. 3.

As a next step, we focus on the solutions of (2.9) that satisfy the initial condition (2.10). These solutions also form a three-dimensional manifold, which we denote by M^0. In two stages, we track the solutions on M^0 from $\xi = 0$ to $\xi = \xi_{\max}$; see Fig. 2. First, in Section 4, we pull M^0 forward to $\xi = \xi_b = k_b \log(\frac{1}{a})$, for some $k_b > 0$. Then, in Sections 5 and 6, we track the solutions on M^0 further forward from $\xi = \xi_b$ to $\xi = \xi_{\max}$; this is the interval in which the bumps lie. We introduce a 'slow' independent variable $\eta = a\xi$ and the shifted phase variable $\phi = \psi + \frac{a\xi}{2}$ in (2.9). Under the assumption that $|\phi| < a^{\frac{1}{2}}$ (this strict inequality is

proved in Section 7), the leading order system becomes

$$\begin{cases} A_\xi = AB \\ B_\xi = 1 - \dfrac{\eta^2}{4} - B^2 - A^2 + aB\left(\dfrac{(1-d)}{\eta} + K\eta\right) + \text{hot} \\ \eta_\xi = a. \end{cases} \tag{2.12}$$

The higher order terms in the equation for B contain the ϕ^2-term.

The global geometry of the invariant manifolds of (2.12) is studied in Section 5. For $a = 0$, the system (2.12) is a planar Hamiltonian system depending on a fixed parameter η. For every $\eta \in (0, 2)$, it has a pair of saddle fixed points connected by a pair of heteroclinic orbits that enclose a family of periodic orbits. For $0 < a \ll 1$, it follows from geometric singular perturbation theory [10,12] that the manifolds persist. Using adiabatic Melnikov function theory we determine the splitting distance between the invariant manifolds and their intersection points.

This global geometric information is then used in Section 6 to track solutions on M^0 further forward to $\eta = \eta_{\max} = a\xi_{\max}$. It follows that, on the cross section $\eta = \eta_{\max}$ in the A–B plane, M^0 exhibits a highly complex structure; see Fig. 8. As an important result, on the cross section $\eta = \eta_{\max}$ in the A–B plane, there are two families of transverse intersection points of the manifolds M^0 and M^∞. Hence, there exist two families of solutions on M^0 and M^∞ such that for each member of these families the A and B coordinates are the same at $\eta_{\max}$ (values different for each member, of course). The properties of these solutions are further specified in Section 8. We note here that one of the main properties is that the A coordinates at $\xi_{\max}$ of the intersection points lie exponentially close to zero for one family while they are $\mathcal{O}(a^{\frac{3}{8}})$ for the other family.

With the above analysis the proof of Theorem 2.1 is almost finished. The last step concerns the ψ coordinates. In general, the ψ coordinates of the solutions just identified need not coincide. In Section 9, we show that the interval of values of the ψ coordinates of the relevant points on M^0 overlaps the interval of values of the ψ coordinates of the relevant points on M^∞. Furthermore, we prove that the derivative of the ψ coordinate with respect to d of points on M^0 is much larger than that same derivative for points on M^∞; see Fig. 10 for a sketch of the manifolds in the d–ψ plane. Therefore, we can conclude that, for each member of the two families identified above and for each a sufficiently small, there exists a unique d such that not only are the A and B coordinates of the solutions on both manifolds the same but also their ψ coordinates are the same. Concluding, the above analysis shows that the three-dimensional manifolds M^0 and M^∞ have two families of transverse intersection points in the A–B–ψ–ξ–d five-dimensional phase space and, hence, that the locally unique, multi-bump solutions stated in Theorem 2.1 exist.

Remark 2.2. In the proofs throughout this article, the letter c is used to denote various positive, $\mathcal{O}(1)$ constants. These constants are local.

3. Tracking M^∞ backward to $\xi = \frac{\sqrt{2}}{a\sqrt{a}}$

The behaviour of solutions of the NLS on M^∞ for ξ very large was already studied in [15,20,21]. The results can be extended to the GL and are stated in the following theorem:

Theorem 3.1. *Assume that $2 < d < 4$ is fixed and that a is sufficiently small. Then for every $\xi \geq \frac{\sqrt{2}}{a\sqrt{a}}$ and A_1 sufficiently small, there is a unique solution to (2.9) that satisfies the boundary condition (2.11) and $A(\xi) = A_1$.*

The proof of this theorem is an application of the contraction mapping principle to a rescaled form of system (2.9). It is a straightforward extension of Theorem 3.1 in [20]; therefore, we will not give it here, and instead we refer the reader to [20].

Theorem 3.1 gives us a solution satisfying the boundary condition (2.11) that is characterised by its amplitude at $\xi_1 = \frac{\sqrt{2}}{a\sqrt{a}}$ and the value of d. Hence, choosing $A(\xi_1)$ and d gives a locally unique solution that is a function of ξ. Thus, the manifold M^∞ of solutions that satisfy the boundary condition is of dimension 3 in (A, B, ψ, ξ, d)-space.

3.1. Tracking M^∞ backward further to $\xi_{\max} = \frac{2-\sqrt{a}}{a}$

In this section, we analyse the behaviour of the solutions on M^∞ as they are integrated backward further from $\xi_1 = \frac{\sqrt{2}}{a\sqrt{a}}$ to $\xi_{\max} = \frac{2-\sqrt{a}}{a}$. We extend the method used in [21] for the NLS to the GL. However, the extension of the results to the GL is not straightforward and does lead to a different statement for ψ at $\xi_{\max}$; therefore, we do give this analysis here.

We denote the values of A, B, and ψ at $\xi = \xi_{\max}$ by $A_d^\infty(\xi_{\max})$, $B_d^\infty(\xi_{\max})$, and $\psi_d^\infty(\xi_{\max})$. We will show that $B_d^\infty(\xi_{\max})$ lies close to $-a^{\frac{1}{4}}$ in a C^1 manner (see Lemmas 3.2 and 3.5) and that $\psi_d^\infty(\xi_{\max})$ lies close to $\frac{-a\xi_{\max}}{2}$ (see Lemma 3.2). Moreover, for these solutions, the interval of values that $A_d^\infty(\xi_{\max})$ can reach stretches to include the interval $(0, a^{\frac{3}{8}}]$. In Fig. 3, a sketch of the manifold M^∞ is given in the A–B plane.

In the same way as in [15,20,21], we introduce a rescaling of Q for which the linearised equation (2.5) for Q becomes self-adjoint. Let $Q(\xi) = X(\xi)W(\xi)$, where X is chosen so that, after substitution in (1.3), the equation for W does not contain any first-order derivatives (i.e., the linearised equation for W is self-adjoint). This gives $X(\xi) = \mathrm{e}^{-\frac{\mathrm{i}a}{4}\xi^2}\xi^{\frac{1-d}{2}}$ and the following equation for W:

$$(1-\mathrm{i}Ka)W_{\xi\xi} + \left[\frac{a^2\xi^2}{4} - 1 - \frac{\mathrm{i}a}{2}(d-2) - \frac{1}{4\xi^2}(d-1)(d-3) + \mathrm{i}Ka\left(\frac{\mathrm{i}a}{2} + \frac{a^2\xi^2}{4} + \frac{1}{4\xi^2}(d-1)(d-3)\right)\right]W + (1+\mathrm{i}bKa)\xi^{1-d}|W|^2W = 0. \tag{3.1}$$

The linearised version of this equation reduces for $0 < a \ll 1$ and $\xi \gg 1$ to the parabolic cylinder equation

$$W_{\xi\xi} + \left(\frac{a^2\xi^2}{4} - 1\right)W = 0. \tag{3.2}$$

At $\xi = \frac{2}{a}$ the type of Eq. (3.2) changes from elliptic for $\xi > \frac{2}{a}$ to hyperbolic for $\xi < \frac{2}{a}$ since the coefficient in front of the W-term vanishes there.

For $\xi \gg \frac{2}{a}$, the two linearly independent solutions of (3.2) are given to leading order by

$$W_1 = \xi^{\frac{d-3}{2}-\frac{\mathrm{i}}{a}}\mathrm{e}^{\frac{\mathrm{i}a}{4}\xi^2} \quad \text{and} \quad W_2 = \xi^{\frac{1-d}{2}+\frac{\mathrm{i}}{a}}\mathrm{e}^{\frac{-\mathrm{i}a}{4}\xi^2}.$$

The higher order terms are small as long as $\xi \gg \frac{2}{a}$ and $a \ll 1$. Solution W_2 does not satisfy condition (2.7); hence, it is not the solution that we are looking for (see Section 2). Instead, W_1 has the correct asymptotics at infinity; it does satisfy condition (2.7).

To determine approximations for $B_d^\infty(\xi_{\max})$ and $\psi_d^\infty(\xi_{\max})$, we study solutions of (3.2) close to the turning point to obtain an estimate for the linearised equation (2.5). We denote these approximations by $B_{d,\mathrm{lin}}^\infty(\xi_{\max})$ and $\psi_{d,\mathrm{lin}}^\infty(\xi_{\max})$. Then, we extend these results to the full nonlinear equation (1.3) for Q; see Lemma 3.2.

Lemma 3.1. *For $d > 2$ fixed and for a sufficiently small,*

$$B_{d,\mathrm{lin}}^\infty(\xi_{\max}) = -a^{\frac{1}{4}} + \frac{1}{4}\sqrt{a} + hot,$$
$$\psi_{d,\mathrm{lin}}^\infty(\xi_{\max}) + \frac{a\xi_{\max}}{2} \quad \textit{is exponentially small.}$$

This lemma follows from the explicit expression for the leading order solution of (3.2) and the relations between A, B, ψ, and W,

$$\begin{aligned} A &= |Q| = \xi^{\frac{1-d}{2}}|W|, \\ B &= \mathrm{Re}\left(\frac{W_\xi}{W}\right) + \frac{1-d}{2\xi}, \\ \psi &= \mathrm{Im}\left(\frac{W_\xi}{W}\right) - \frac{a\xi}{2}. \end{aligned} \tag{3.3}$$

See Lemma 3.1 and Appendix A in [21] for a detailed proof.

Next, we extend these approximations to the solutions of the full equation (3.1), and hence, to Eq. (1.3).

Lemma 3.2. *For $d > 2$ fixed and for a sufficiently small, there exist positive constants c_1 and c_2 such that*

$$B_d^\infty(\xi_{\max}) = -a^{\frac{1}{4}} + c_1\sqrt{a} \quad \textit{and}$$
$$\psi_d^\infty(\xi_{\max}) = -\frac{a\xi_{\max}}{2} + c_2a^{d-\frac{1}{2}}(1+b).$$

Proof. We introduce amplitude and phase coordinates associated with W,

$$W(\xi) = y(\xi)\exp\left[\mathrm{i}\int_0^\xi \phi(x)\mathrm{d}x\right], \qquad z(\xi) = \frac{y_\xi}{y}. \tag{3.4}$$

These are analogous to the coordinates A, B, and ψ associated with Q. Moreover, (3.3) and (3.4) imply the following relations between B and z and between ψ and ϕ:

$$\begin{aligned} z &= \frac{d-1}{2\xi} + B, \\ \phi &= \frac{a\xi}{2} + \psi. \end{aligned} \tag{3.5}$$

Eq. (3.1) may be written in the variables y, z, and ϕ as

$$\begin{cases} y_\xi = yz \\ z_\xi = -z^2 + \phi^2 + \dfrac{1}{4\xi^2}(d-1)(d-3) + \dfrac{1}{(1+a^2K^2)}\left[1 - \dfrac{a^2\xi^2}{4}(1-a^2K^2) - (1-ba^2K^2)\xi^{1-d}y^2 \right. \\ \qquad \left. - \dfrac{a^2K}{2}(d-3)\right] \\ \phi_\xi = -2\phi z + \dfrac{a}{1+a^2K^2}\left[\dfrac{1}{2}(d-2) + \dfrac{a^2K^2}{2} + K\left(1 - \dfrac{a^2\xi^2}{2}\right) - K\xi^{1-d}y^2(1+b)\right]. \end{cases} \tag{3.6}$$

We will compare the solutions of system (3.6) to the solutions of the linear equation for W obtained in Lemma 3.1. Let $\hat{z}(\xi) = z(\xi) - \bar{z}(\xi)$ and $\hat{\phi}(\xi) = \phi(\xi) - \bar{\phi}(\xi)$, where $\bar{z}(\xi)$ and $\bar{\phi}(\xi)$ are the solutions of the linearised version of Eq. (3.1). Note that in the amplitude and phase coordinates linearisation corresponds to setting $y = 0$, so the linearised system depends only on z and ϕ. The estimates for B and ψ in Lemma 3.1 imply that $\bar{z} = -a^{\frac{1}{4}} + \frac{1}{4}\sqrt{a}$ and $\bar{\phi}$ is exponentially small to leading order at $\xi = \xi_{\max}$. Here we will show that $|\hat{z}| < a^{d-\frac{3}{2}} < \sqrt{a}$ and that $|\hat{\phi}| < c_2(1+b)a^{d-\frac{1}{2}}$ for $\xi \geq \xi_{\max}$. Combining these two results, we find approximations for z and ϕ. Finally, via (3.5), this leads to the desired approximations for B and ψ.

The system (3.6) can be written in terms of y, $\hat{z}$, and $\hat{\phi}$ as

$$\begin{aligned} &y_\xi = y\bar{z} + y\hat{z} \\ &\begin{pmatrix} \hat{z}_\xi \\ \hat{\phi}_\xi \end{pmatrix} = \begin{pmatrix} -2\bar{z} & 2\bar{\phi} \\ -2\bar{\phi} & -2\bar{z} \end{pmatrix}\begin{pmatrix} \hat{z} \\ \hat{\phi} \end{pmatrix} + \begin{pmatrix} \hat{\phi}^2 - \hat{z}^2 - \dfrac{1-ba^2K^2}{1+a^2K^2}\xi^{1-d}y^2 \\ -2\hat{\phi}\hat{z} - \dfrac{(1+b)Ka}{1+a^2K^2}\xi^{1-d}y^2 \end{pmatrix}. \end{aligned} \tag{3.7}$$

The $\hat{z}$- and $\hat{\phi}$-equations have been written in this way to show the structure of the 2×2-matrix, whose behaviour plays an important role in the analysis.

For $\xi \gg \frac{2}{a}$ we have that $\bar{z} \sim -\frac{3-d}{2\xi} < 0$ (because $\bar{z} = \operatorname{Re}\frac{\frac{\mathrm{d}}{\mathrm{d}\xi}|W|}{|W|}$ from the definition of the polar coordinates (3.4) and because we evaluate along W_1). We need that $\bar{z} \leq 0$ for every $\xi \geq \xi_{\max}$. For $\xi \gg 1$ and $a \ll 1$, the solutions to (3.2) can be used to calculate the sign of $\bar{z}$. A solution to (3.2) can be written as

$$W = K_1 W\left(\frac{1}{a}, \sqrt{a}\xi\right) + \frac{\mathrm{i}}{2}\mathrm{e}^{-\frac{\pi}{a}} W\left(\frac{1}{a}, -\sqrt{a}\xi\right),$$

where the functions on the right hand side are Weber parabolic functions, see [1], and K_1 is a constant. Computation of $\bar{z} = \operatorname{Re}\frac{\frac{\mathrm{d}}{\mathrm{d}\xi}|W|}{|W|}$ shows that $\bar{z} < 0$ at $\xi = \frac{2}{a}$ (for $a \ll 1$), and $\bar{z}$ decreases monotonically and algebraically to 0 as ξ increases, so $\bar{z} < 0$ for $\xi \geq \xi_{\max}$.

Define $\xi_2 < \xi_1 = \frac{\sqrt{2}}{a\sqrt{a}}$ by $\bar{z}(\xi_2) = -2a$. Such a ξ_2 exists because $\bar{z} \sim -a^{-\frac{1}{4}}$ at $\xi_{\max}$, $\bar{z}$ increases monotonically for $\xi \geq \xi_{\max}$, and $\bar{z} \sim -(\frac{3-d}{2\sqrt{2}})a^{3/2}$ at ξ_1. It remains to show that, for $y(\xi_1)$ in some appropriate range, $|\hat{z}| < \sqrt{a}$ and $|\hat{\phi}| < c_2(1+b)a^{d-\frac{1}{2}}$ for $\xi \geq \xi_{\max}$.

To show this, we need the following

Lemma 3.3. *We denote by $\mathcal{V}$ the space of solutions to (3.7) that satisfy*

a. $(y, \hat{z}, \hat{\phi})$ *is exponentially small for* $\xi_2 \leq \xi \leq \xi_1$,
b. $|y| < 2a^{-\frac{1}{8}}$, $|\hat{z}| < \sqrt{a}$, *and* $|\hat{\phi}| < c_2(1+b)a^{d-\frac{1}{2}}$ *for* $\xi \geq \xi_{\max}$.

Then for $y(\xi_1)$ chosen appropriately, sufficiently small, the solutions remain in this space.

The proof of this lemma is given in Appendix A, and it is based on an argument that uses continuous induction. The fact that solutions satisfy the first property of the space can be proved by showing that the two following statements hold.

First, we show that if $y(\xi)$ is exponentially small for $\xi \geq \xi_2$, then $\hat{z}$ and $\hat{\phi}$ are exponentially small for $\xi \geq \xi_2$, provided that they are already this small at $\xi = \xi_1$. Vice versa, we need to show that if $\hat{z}$ is exponentially small for $\xi \geq \xi_2$ and y is exponentially small at ξ_1, then for $y(\xi_1)$ chosen small, y is also exponentially small for $\xi \geq \xi_2$. The same type of argument can be used to show that the solutions also satisfy property b.

Applying this lemma, we can finish the proof of Lemma 3.2. We choose $y(\xi_1)$ so that Lemma 3.3 is satisfied. Then it follows immediately that $|\hat{\phi}| < c_2(1+b)a^{d-\frac{1}{2}}$ and $|\hat{z}| < \sqrt{a}$ for every $\xi \geq \xi_{\max}$. □

In the following lemma, we estimate $A_d^\infty(\xi_{\max})$.

Lemma 3.4. *For $d > 2$ fixed and for a sufficiently small, the range of $A_1 = A(\frac{\sqrt{2}}{a\sqrt{a}})$ can be chosen such that, as a function of A_1, $A_d^\infty(\xi_{\max})$ is onto $(0, a^{\frac{3}{8}}]$.*

Proof. We use the relation $A = \xi^{\frac{1-d}{2}} y$, between y and A that follows from the relation between Q and W. The proof of Lemma 3.2 shows that one may choose the range of $y(\xi_1)$ such that $y < 2a^{-\frac{1}{8}}$ for all $\xi \geq \xi_{\max}$. In the proof of Lemma 3.2, we chose $y(\xi_1)$ in an interval such that $y(\xi_2)$ is exponentially small. For the largest value of $y(\xi_1)$ we know that $y(\xi_{\max}) > \sqrt{2}a^{-\frac{1}{8}}$. Thus $A_d^\infty(\xi_{\max}) > a^{\frac{3}{8}}$ since $\xi_{\max}^{\frac{1-d}{2}} > \sqrt{\frac{a}{2}}$. □

We conclude this section with a lemma extending the C^0 closeness of $B_d^\infty(\xi_{\max})$ to $-a^{1/4}$ in the A–B plane to C^1 closeness. This result will then be used below in Section 6 to establish the transversality of M^0 and M^∞.

Lemma 3.5. *For $d > 2$ fixed, a sufficiently small, and for each A_1 in the range of A_1 values found in Lemma 3.4, the map*

$$A_1 \to \left(A_d^\infty(\xi_{\max}, A_1), B_d^\infty(\xi_{\max}, A_1)\right)$$

has a slope that is less than $ca^{\frac{1}{8}}$ in the A–B plane for some $c > 0$.

Proof. Define $Z = \frac{\partial z}{\partial A_1}$, $Y = \frac{\partial y}{\partial A_1}$, and $\Psi = \frac{\partial \phi}{\partial A_1}$. Then Z, Y, and Ψ satisfy the variational equations

$$Y_\xi = (\bar{z} + \hat{z})Y + yZ,$$

$$\begin{pmatrix} Z_\xi \\ \Psi_\xi \end{pmatrix} = \begin{pmatrix} -2\bar{z} & 2\bar{\phi} \\ -2\bar{\phi} & -2\bar{z} \end{pmatrix} \begin{pmatrix} Z \\ \Psi \end{pmatrix} + \begin{pmatrix} 2\hat{\phi}\Psi - 2\hat{z}Z - 2\dfrac{1 - ba^2K^2}{1 + a^2K^2}\xi^{1-d}Yy \\ -2\hat{\phi}Z - 2\hat{z}\Psi - 2\dfrac{(1+b)Ka}{1 + a^2K^2}\xi^{1-d}Yy \end{pmatrix}. \tag{3.8}$$

Since Y stays bounded away from 0, we may look at the quantities Z/Y and Ψ/Y. These satisfy the equations

$$\begin{pmatrix} (Z/Y)_\xi \\ (\Psi/Y)_\xi \end{pmatrix} = \begin{pmatrix} -3\bar{z} - 3\hat{z} & 2\bar{\phi} + 2\hat{\phi} \\ -2\bar{\phi} - 2\hat{\phi} & -3\bar{z} - 3\hat{z} \end{pmatrix} \begin{pmatrix} Z/Y \\ \Psi/Y \end{pmatrix} - \begin{pmatrix} y(Z/Y)^2 + 2\dfrac{1 - ba^2K^2}{1 + a^2K^2}\xi^{1-d}y \\ y(Z/Y)(\Psi/Y) + 2\dfrac{(1+b)Ka}{1 + a^2K^2}\xi^{1-d}y \end{pmatrix}.$$

Integrating backward to $\xi_{\max}$ and using an appropriate integrating factor similar to that in the proof of Lemma 3.3, we have that Z/Y can be estimated by $ca^{-\frac{1}{4}}\xi^{1-d}y\frac{1-ba^2K^2}{1+a^2K^2}$ (since $\bar{z}$ dominates $\hat{z}$ and $\bar{z} \approx -a^{-\frac{1}{4}}$ and negative for $\xi \geq \xi_{\max}$) and Ψ/Y by $ca^{-\frac{1}{4}}\xi^{1-d}y\frac{(1+b)Ka}{1+a^2K^2}$. Also, we know that $y < 2a^{-\frac{1}{8}}$. Therefore, $(\frac{\partial z}{\partial A_1})/(\frac{\partial y}{\partial A_1}) = Z/Y \leq c\xi^{1-d}ya^{-\frac{1}{4}}\frac{1-ba^2K^2}{1+a^2K^2}$, and so $(\frac{\partial B}{\partial A_1})/(\frac{\partial A}{\partial A_1}) \leq ca^{-\frac{1}{4}}\xi^{\frac{1-d}{2}}y\frac{1-ba^2K^2}{1+a^2K^2} \leq ca^{\frac{4d-7}{8}} \ll ca^{\frac{1}{8}}$ for some positive constant c. □

Remark 3.1. More generally, we can pull back M^∞ to a point $\xi = \frac{2-b}{a}$, where $a^{\frac{2}{3}} \ll b \ll a^{\frac{2}{5}}$. The choice of $b = \sqrt{a}$, used to obtain $\xi_{\max}$, was made to simplify the analysis. Further details are given in Remark 6.1, after the necessary analysis of M_0 is presented.

4. The manifold M^0 satisfying the initial conditions

In this section, we will study solutions of the system (2.9) that satisfy the initial conditions (2.10). Moreover, we choose $A(0)$ close to zero but positive. We construct a manifold M^0 of such solutions and track it forward to $\xi = \xi_b$. We denote the values of A, B and ψ at $\xi = \xi_b$ by $A_d^0(\xi_b)$, $B_d^0(\xi_b)$ and $\psi_d^0(\xi_b)$. We show that $B_d^0(\xi_b)$ lies in an interval where $B = 1$ to leading order. Also, we show that there exists an interval of initial conditions for A such that A at $\xi = \xi_b$ overlaps the interval $(0, ca]$. Finally, we will prove that, at $\xi = \xi_b$, the image of the curve of these solutions lies horizontally in the (A, B)-plane.

The solutions that we construct here lie close to the zero solution of (1.6). Therefore, we first study the solutions to Eq. (1.6) and then we use the fact that the solutions of system (2.9) lie close to Eq. (1.6).

4.1. The estimates on $B_d^0(\xi_b)$

We want to study solutions that lie close to a solution of Eq. (1.6); therefore, we analyse this equation first and write it as a first-order system. We introduce $T = \frac{R_\xi}{R}$ so that (1.6) becomes

$$\begin{cases} R_\xi = RT \\ T_\xi = \dfrac{1-d}{\xi}T - T^2 - R^2 + 1. \end{cases} \tag{4.1}$$

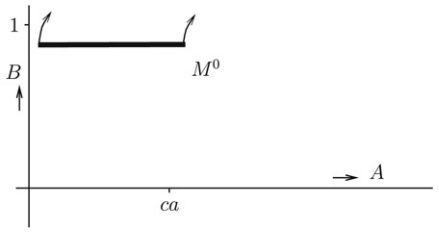

Fig. 4. A sketch of the manifold M^0 in the A–B plane at $\xi = \xi_b$.

Note that this system is identical to (2.9) if we set $a = 0$ and $\psi = 0$. For large ξ, $1 \ll \xi < \xi_b$, (4.1) has a critical point located to leading order at $R = 0$, $T = 1$. This point is a saddle, and therefore solutions with initial conditions near the zero solution will go towards and then diverge from this solution for large ξ.

From the asymptotics, it follows that a solution to (2.9) that satisfies the initial conditions (2.10) has a ψ-component that remains close to $\psi = -\frac{a\xi}{2}$. Therefore, we introduce $\phi = \psi + \frac{a\xi}{2}$. Note that this is the same ϕ as was used in the previous section; however, the reason why it is used here is different. The system (2.9) then becomes

$$\begin{cases} A_\xi = AB \\ B_\xi = \dfrac{1-d}{\xi}B - B^2 + \dfrac{a^2\xi^2}{4} + \phi^2 - a\xi\phi + \dfrac{1}{1+a^2K^2}\left\{1 - (1 - ba^2K^2)A^2 + a\xi\phi - \dfrac{a^2\xi^2}{2} + a^2K(1+\xi B)\right\} \\ \phi_\xi = \dfrac{1-d}{\xi}\phi - 2\phi B + a\xi B + \dfrac{ad}{2} + \dfrac{a}{1+a^2K^2}\left\{-1 - \xi B + K\left[1 + a\xi\phi - \dfrac{a^2\xi^2}{2} - (1+b)A^2\right]\right\}. \end{cases} \tag{4.2}$$

In this section, we prove that solutions starting in $B(0) = 0$, $\phi(0) = 0$ and $A(0) \in (0, c_r a^{m_r}]$, $m_r > 0$, will evolve into a curve at $\xi = \xi_b$ where $0 < A(\xi_b) < ca^m$, $m > 0$, and B is close to 1; see Fig. 4. We start by showing that the statement holds when setting $\phi = a = 0$ in (4.2).

Hence, we first show that it is true for R and T in (4.1) and then extend this result to the full (A, B, ϕ)-system. For this second step, we prove that ϕ remains small for $0 < \xi < \xi_b$ and then use that (4.2) is a small perturbation of (4.1).

Lemma 4.1. *There exist constants $0 < k_3 < k_4 < k_b$ such that solutions that satisfy $R(0) \in (0, c_r a^{m_r}]$, $T(0) = 0$ evolve at $\xi = \xi_b$ into a curve with*

$$1 - \frac{d-1}{2k_3 \log\left(\frac{1}{a}\right)} < T(\xi_b) < 1 - \frac{d-1}{2k_4 \log\left(\frac{1}{a}\right)} < 1$$

and $0 < R(\xi_b) < ca^{m_r - k_b} = ca^m$. Moreover, for $m_r - k_b = m > 0$, $T_\xi > 0$ and $R_\xi > 0$ for all $0 \le \xi \le \xi_b$.

The proof of this lemma is given in Appendix B.

Now, we will extend the above results to A and B. For that we want to bound ϕ at $\xi = \xi_b$. In order to establish such a bound, we need:

Lemma 4.2. *A solution that satisfies the initial conditions $B(0) = 0$ and $\phi(0) = 0$, i.e. $\psi(0) = 0$, can be represented as*

$$\begin{aligned} \phi(x) &= \psi(x) + \frac{ax}{2} \\ &= \frac{ax^{1-d}}{A^2(x)(1+a^2K^2)}\int_0^x A^2(y)y^{d-1}\left[\frac{d-2+2K+a^2K^2d}{2}\right. \\ &\quad \left. - aK(b+1)A^2(y) + a^2Ky\left(\phi - \frac{ay}{2}\right) + a^3K^2yB(y)\right]\mathrm{d}y \\ &= \frac{xa^3K^2}{2(1+a^2K^2)} + \frac{ax^{1-d}}{A^2(x)(1+a^2K^2)}\int_0^x A^2(y)y^{d-1}\left[\frac{d-2+2K}{2} - aK(b+1)A^2(y) + aKy\left(\phi - \frac{ay}{2}\right)\right]\mathrm{d}y \\ &= \frac{xa^3K^2}{2(1+a^2K^2)} + \frac{ax^{1-d}}{A^2(x)(1+a^2K^2)}I, \end{aligned} \tag{4.3}$$

where

$$I(x) = \int_0^x R(y)A^2(y)y^{d-1}\mathrm{d}y$$

and

$$R(y) = \frac{d-2+2K}{2} - K(b+1)A^2(y) + Kay\left(\phi - \frac{ay}{2}\right).$$

The proof of this lemma is given in Appendix C. Using the explicit expression (4.3) for ϕ, we can now approximate ϕ at $\xi = \xi_b$ as follows:

Lemma 4.3. *For $B(\xi) > 0$ (so that $A_\xi > 0$) and $A(\xi) \leq \tilde{c}$ for $\xi \leq \xi_b$, there exists a constant $C > 0$ such that $|\phi(\xi)| < Ca^p$ for every $0 < p < 1$ and $0 \leq \xi \leq \xi_b$.*

Proof. We will bound the expression I in Eq. (4.3) by studying the different integrals separately. Since A and x^{d-1} are both increasing functions on $0 \leq y \leq \xi \leq \xi_b$ it follows that

$$\int_0^\xi A^2(x)x^{d-1}\mathrm{d}x \leq A^2(\xi)\int_0^\xi x^{d-1}\mathrm{d}x = A^2(\xi)\frac{\xi^d}{d}$$

and similarly

$$\int_0^\xi A^4(x)x^{d-1}\mathrm{d}x \leq A^4(\xi)\frac{\xi^d}{d} \quad \text{and} \quad \int_0^\xi A^2(x)x^{d+1}\mathrm{d}x \leq A^2(\xi)\frac{\xi^{d+2}}{d+2}.$$

The part in I which contains a term ϕ can be estimated by using continuous induction. Assuming $|\phi(x)| < Ca^p$ for $0 \leq x < \xi$, we can bound the integral as follows:

$$\left|\int_0^\xi A^2(x)x^d\phi\mathrm{d}x\right| < Ca^p\int_0^\xi A^2(x)x^d\mathrm{d}x \leq \frac{C_1a^p}{d+1}\xi^{d+1}A^2(\xi).$$

Hence

$$|I(\xi)| \leq A^2(\xi)\xi^d\left[\frac{d-2+2K}{2d} + K\frac{b+1}{d+2}A^2(\xi) + Ka\xi\left(\frac{C_1a^p}{d+1} + \frac{a\xi}{2(d+2)}\right)\right] < CA^2(\xi)\xi^d,$$

where for the second inequality we use the fact that $a\xi \leq a\xi_b = ak_b\log\frac{1}{a} \ll 1$ together with the assumption that $A(\xi) \leq \tilde{c}$.

Substituting this bound into (4.3), we find that

$$|\phi(\xi)| \leq \frac{a\xi}{1+a^2K^2}\left[\frac{a^2K^2}{2} + C\right] < Ca\xi \ll Ca^p$$

for $0 < p < 1$, since $\xi_b \ll a^{-p_1}$ for every $p_1 > 0$. □

As a last step we will show that the results as stated in Lemma 4.1 also hold for A and B.

Lemma 4.4. *There exist constants $k_1, k_2 > 0$ such that for solutions with $A(0) \in (0, c_ra^{m_r}]$, $B(0) = 0$ and $\phi(0) = 0$ the following holds:*

$$1 - \frac{d-1}{2k_1\log\left(\frac{1}{a}\right)} < B(\xi_b) < 1 - \frac{d-1}{2k_2\log\left(\frac{1}{a}\right)} < 1,$$

and $0 \leq A(\xi_b) < c_ra^{m_r-k_b} = c_ra^m$. Furthermore, for $m = m_r - k_b > 0$, $A_\xi > 0$, $B_\xi > 0$ for all $0 \leq \xi \leq \xi_b$.

Proof. We use the fact that A and B lie close to R and T. Using that $B < 1$, it follows analogously to the estimate for R that $0 < A(\xi_b) < c_ra^{m_r-k_b}$. Since a and ϕ are small, the equations for A and B are small perturbations of the equations for R and T. Hence, $B(\xi_b)$ also lies, in a similar way to T, close to $B = 1$. Now, we prove that on the interval at $\xi = \xi_b$, $B_\xi > 0$. The extra terms that the equation for B_ξ in (4.2) contains compared to the equation for T_ξ are given by

$$E_1 = \phi^2 + \frac{a^2}{1+a^2K^2}\left[K^2(1+b)A^2 - aK^2\xi\phi + K(1+\xi B) + (a^2K^2-1)\frac{\xi^2}{4} - K^2\right].$$

We know that $a\xi\phi < a^2$, and since $\xi < \xi_b$, $a^2\xi^2 < a^{\frac{3}{2}}$; hence, $|E_1| \ll \frac{1}{\log\frac{1}{a}}$. Therefore, this term is at $\xi = \xi_b$ much smaller than the other terms which are of order $\frac{1}{\log\frac{1}{a}}$. Hence, $B_\xi > 0$ at $\xi = \xi_b$. □

Remark 4.1. In Section 6 we need that $A_d^0(\xi_b)$ stretches out up to ca. More specifically, $A_d^0(\xi_b)$ must overlap the interval $(0, ca]$ including exponentially small terms. Therefore, we choose $m < 1$ which leads together with the fact that $A_\xi > 0$ for all $0 < \xi < \xi_b$ to the required right boundary. It also follows from the fact that

$$A(\xi_b) = A(0)\mathrm{e}^{\int_0^{\xi_b} B(y)\mathrm{d}y} \leq A(0)a^{-k_b}$$

that if $A(0)$ is exponentially small, this is also true for $A(\xi_b)$.

4.2. The slope in the (A, B)-plane

In this section, we show that, at $\xi = \xi_b$, the image of the curve of initial conditions I_0 lies horizontally. We use the variational equations of system (4.2):

$$\begin{cases} \hat{A}_\xi = B\hat{A} + A\hat{B} \\ \hat{B}_\xi = \dfrac{1-d}{\xi}\hat{B} - 2B\hat{B} + 2\phi\hat{\phi} - a\xi\hat{\phi} + \dfrac{1}{1+a^2K^2}(-2(1-ba^2K^2)A\hat{A} + a\xi\hat{\phi} + a^2K\xi\hat{B}) \\ \hat{\phi}_\xi = \dfrac{1-d}{\xi}\hat{\phi} - 2\phi\hat{B} - 2B\hat{\phi} + a\xi\hat{B} + \dfrac{a}{1+a^2K^2}(-\xi\hat{B} + K[a\xi\hat{\phi} - 2(1+b)A\hat{A}]), \end{cases}$$

where $\hat{A}$, $\hat{B}$ and $\hat{\phi}$ are the tangent vectors. As in Lemma 3.5 we compute the slope of the curve by using projectivised quantities. We define $u = \frac{\hat{B}}{\hat{A}}$ and $v = \frac{\hat{\phi}}{\hat{A}}$. The functions u and v satisfy

$$\begin{cases} u_\xi = u\left[\dfrac{1-d}{\xi} - 3B - Au + \dfrac{a^2K\xi}{1+a^2K^2}\right] + v\left[2\phi - \dfrac{a^3K^2\xi}{1+a^2K^2}\right] - \dfrac{2}{1+a^2K^2}(1-ba^2K^2)A \\ v_\xi = v\left[\dfrac{1-d}{\xi} - 3B - Au + \dfrac{a^2K\xi}{1+a^2K^2}\right] + u\left[-2\phi + \dfrac{a^3K^2\xi}{1+a^2K^2}\right] - 2a\dfrac{(1+b)K}{1+a^2K^2}A. \end{cases} \tag{4.4}$$

The slope that we are interested in is represented by the value of u at $\xi = \xi_b$. We will show that u is small at $\xi = \xi_b$ so that the image of I_0 lies approximately horizontal in the (A, B)-plane. This is stated in

Lemma 4.5. *For a sufficiently small and $d > 2$, the image of the trajectories produced in Lemma 4.4 has, in the (A, B)-plane, a slope that is less than ca^l for some $c > 0$ and $0 < l < 1$.*

The proof of this lemma will be given in Appendix C.1. The results of this lemma imply that, in the (A, B)-plane, the slope of the graph is smaller than ca^l where $0 < l < 1$ and, hence, it lies approximately horizontally; see Fig. 4.

5. Structure of the invariant manifolds of system (2.12)

In this section, we study the system (2.12) for $\eta > \eta_{\min} = a\xi_b$, and we establish an asymptotic approximation for the position of M_0 at $\eta = \eta_{\max} = a\xi_{\max}$. Along the lines of [21] we start by studying the geometry of system (2.12) for $a = 0$ and then apply the Fenichel theory to obtain the relevant information about the geometry for $0 < a \ll 1$. Finally, by introducing an adiabatic Melnikov function, we obtain a more detailed view of the structure of the invariant manifolds of system (2.12) for $0 < a \ll 1$.

5.1. Geometry of the system (2.12) with $a = 0$

For $a = 0$, the geometry of the system (2.12) is the same as in the analysis of the NLS equation; see [21]. Here we summarise. When $a = 0$, there exist three curves of fixed points,

$$\Gamma_\pm^0 = \left\{ (A, B, \eta) \,\middle|\, A = 0, B = \pm\sqrt{1 - \frac{\eta^2}{4}}\,, \eta_{\min} < \eta < \eta_{\max} \right\} \tag{5.1}$$

and

$$\Gamma_0 = \left\{ (A, B, \eta) \,\middle|\, A = \sqrt{1 - \frac{\eta^2}{4}},\ B = 0, \eta_{\min} < \eta < \eta_{\max} \right\}; \tag{5.2}$$

see Fig. 5(a). The curves $\Gamma_\pm^0$ are normally hyperbolic manifolds, since they are the unions of saddle fixed points $(A, B) = (0, \pm\sqrt{1 - \frac{\eta^2}{4}})$ for every fixed η; see Fig. 5(a). These saddles are connected by a heteroclinic orbit for every $\eta \in (\eta_{\min}, \eta_{\max})$.

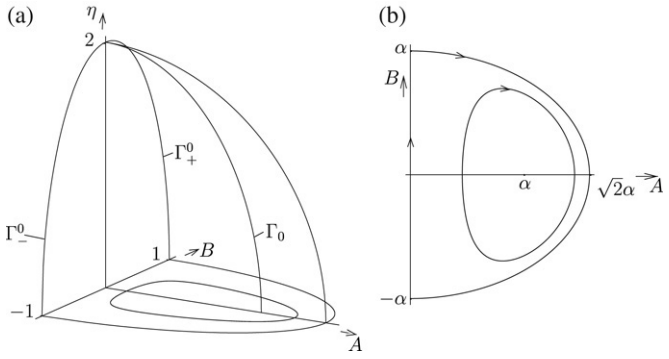

Fig. 5. (a) A sketch of the three curves of critical points $\Gamma^0_\pm$ and Γ_0 in the A–B–η plane for $a = 0$. Here the positive B-axis points into the paper. (b) The flow in the A–B plane for $\eta \in (\eta_{\min}, \eta_{\max})$ fixed, where $\alpha = \sqrt{1 - \frac{\eta^2}{4}}$.

For every fixed η, there exists a one-parameter family of periodic orbits in the domain inside the heteroclinic orbit. This family limits on the centre fixed point $(A, B) = (A_{ctr}, 0) = (\sqrt{1 - \frac{\eta^2}{4}}, 0)$, see Fig. 5(b), and the curve Γ_0 shown in Fig. 5(a) is the union of these centres.

The leading part of system (2.12) can be written as the Duffing equation

$$A_{\xi\xi} = A\left(1 - \frac{\eta^2}{4} - A^2\right), \tag{5.3}$$

and hence, explicit expressions can be given for the heteroclinic and periodic orbits, see [11], for example. Note that the variable B used here is the logarithmic derivative of A; see (2.8). For every $\eta_{\min} < \eta < \eta_{\max}$, the heteroclinic orbit is given by

$$(A_0(\xi), B_0(\xi)) = [\sqrt{2}\alpha\,\mathrm{sech}(\alpha\xi), -\alpha\tanh(\alpha\xi)], \tag{5.4}$$

where $\alpha = \sqrt{1 - \frac{\eta^2}{4}}$. We denote the manifold that consists of all these heteroclinic connections with $\eta_{\min} < \eta < \eta_{\max}$ by $\mathcal{W}$. The periodic solutions are given by

$$A^{(k)}(\xi) = \sqrt{2}\beta\,\mathrm{dn}(\beta\xi, k), \tag{5.5}$$

$$B^{(k)}(\xi) = -k^2\beta\frac{\mathrm{sn}(\beta\xi, k)\mathrm{cn}(\beta\xi, k)}{\mathrm{dn}(\beta\xi, k)}, \tag{5.6}$$

where $\beta = \frac{\alpha}{\sqrt{2-k^2}}$ and $0 < k < 1$. Here, $k = 0$ corresponds to the centre point $(A, B) = (\sqrt{1 - \frac{\eta^2}{4}}, 0)$ and $k = 1$ to the heteroclinic solution. The period of such a solution is given by $T_0^{(k)} = 2\frac{K(k)}{\beta}$, where $K(k)$ is the complete elliptic integral of the first kind.

Finally, for system (2.12) with $a = 0$, there exist two integrals:

$$\kappa_1 = \frac{1}{2}A^2B^2 - \frac{1}{2}\left(1 - \frac{\eta^2}{4}\right)A^2 + \frac{1}{4}A^4 \tag{5.7}$$

$$\kappa_2 = \eta.$$

5.2. *Persistence of the invariant manifolds for* $0 < a \ll 1$ *and their transverse intersections*

Since the two curves of critical points $\Gamma^0_\pm$ are normally hyperbolic, we can apply the Fenichel theory [10,12]. Therefore, we find that for $0 < a \ll 1$ and η restricted to $(\eta_{\min}, \eta_{\max})$, the $\Gamma^0_\pm$ persist as slow manifolds Γ_+ and Γ_-, which lie $\mathcal{O}(a)$ close to Γ^0_+ and Γ^0_-, respectively. These manifolds must also still lie in the plane $\{A = 0\}$, since this remains an invariant plane for $a \neq 0$. Furthermore, it follows from the Fenichel theory that the manifolds Γ_+ and Γ_- have stable and unstable manifolds $\mathcal{O}(a)$ close to those of the unperturbed system. The manifolds no longer coincide as they did for $a = 0$. We denote the component of the unstable manifold of Γ_+ that lies $\mathcal{O}(a)$ close to the manifold $\mathcal{W}$ by $W^u(\Gamma_+)$, and the component of the stable manifold of Γ_- that lies $\mathcal{O}(a)$ close to the manifold $\mathcal{W}$ by $W^s(\Gamma_-)$.

Now, we study the behaviour of the unstable manifold of Γ_+, $W^u(\Gamma_+)$, and the stable manifold of Γ_-, $W^s(\Gamma_-)$, for $0 < a \ll 1$. The Melnikov method for slowly varying systems, see [17,22], yields an expression for the distance between $W^u(\Gamma_+)$ and $W^s(\Gamma_-)$ as a function of η. In fact, denoting the first intersection of $W^u(\Gamma_+)$ with the set $\{B = 0, A > 0\}$ by $P(\Gamma_+)$, and similarly the first intersection of $W^s(\Gamma_-)$ with the same set by $P^{-1}(\Gamma_-)$, we find the distance between $P(\Gamma_+)$ and $P^{-1}(\Gamma_-)$.

Remark 5.1. The Fenichel and Melnikov theorems may be used directly to obtain the desired results for all $\eta \in (0, 2)$. Here, we are also interested in the behaviour of $W^u(\Gamma_+)$ and $W^s(\Gamma_-)$ up to $\eta_{\max} = 2 - \sqrt{a}$ and we note that after a suitable rescaling (the eigenvalues are of size $\mathcal{O}(\sqrt{a})$ but the perturbation is of size $\mathcal{O}(a)$) the Fenichel and Melnikov theories can also be applied up to $\eta_{\max}$.

To apply the Melnikov method, we transform system (2.12) by introducing $C = AB$ so that it is explicitly divergence free:

$$\begin{cases} A_\xi = C \\ C_\xi = A\left(1 - \dfrac{\eta^2}{4} - A^2\right) + aC\left(\dfrac{1-d}{\eta} + K\eta\right) + \text{hot} \\ \eta_\xi = a. \end{cases} \tag{5.8}$$

To leading order, system (5.8) is the Duffing equation and in this representation, the plane $B = 0$ corresponds to the plane $C = 0$.

Compared to the corresponding system that was obtained for the NLS equation in [21], this system contains an extra term $aK\eta C$. Along the same lines as in [21], we compute the Melnikov function.

For any η_0 such that $\eta_{\min} < \eta_0 < \eta_{\max}$, we define A_a^u and A_a^s (which depend on η_0) as the intersection points of orbits on $W^u(\Gamma_+)$ and $W^s(\Gamma_-)$, respectively, with $C = 0$ on $\{\eta = \eta_0\}$. The solutions $\gamma_a^u(\xi) = (A_a^u(\xi), C_a^u(\xi), \eta_a^u(\xi))$ in $W^u(\Gamma_+)$ and $\gamma_a^s(\xi) = (A_a^s(\xi), C_a^s(\xi), \eta_a^s(\xi))$ in $W^s(\Gamma_-)$ for the perturbed system (5.8) are determined by the initial condition $\gamma_a^{u,s}(\xi) = (A_a^{u,s}(\xi), 0, \eta_0)$. And $\gamma_0(\xi) = (A_0(\xi), C_0(\xi), \eta_0)$ is the heteroclinic solution of the unperturbed system with $\gamma_0(0) = (\sqrt{2(1 - \frac{\eta_0^2}{4})}, 0, \eta_0)$. Here A_0 and C_0 are given explicitly by (5.4), where $C_0 = A_0 B_0$. We define the following ξ-dependent distance function:

$$\Delta(\xi, \eta_0) = \left\{ \begin{pmatrix} \dfrac{\partial}{\partial a}(A_a^u(\xi) - A_a^s(\xi)) \\ \dfrac{\partial}{\partial a}(C_a^u(\xi) - C_a^s(\xi)) \end{pmatrix} \wedge \begin{pmatrix} C_0(\xi) \\ A_0(\xi)\left(1 - \dfrac{\eta_0^2}{4} - A_0(\xi)^2\right) \end{pmatrix} \right\}.$$

From this ξ-dependent distance function, we derive the adiabatic Melnikov function in the usual way for slowly varying systems, see [22], as

$$\Delta(0, \eta) = \int_{-\infty}^{\infty} \left\{ \begin{pmatrix} 0 \\ C_0\left(\dfrac{1-d}{\eta} + K\eta\right) \end{pmatrix} + \begin{pmatrix} 0 \\ -\dfrac{\eta}{2}A_0 \end{pmatrix} \frac{\partial \eta}{\partial a} \right\} \wedge \begin{pmatrix} C_0 \\ A_0\left(1 - \dfrac{\eta^2}{4} - A_0^2\right) \end{pmatrix} \mathrm{d}\xi.$$

Here $\frac{\partial}{\partial \xi}(\frac{\partial \eta}{\partial a}) = 1$ and $\frac{\partial \eta}{\partial a} = 0$ for $\xi = 0$ and hence $\frac{\partial \eta}{\partial a} = \xi$. Computing the integrals using (5.4) and $C_0 = A_0 B_0$, we find

$$\begin{aligned} \Delta(0, \eta) &= \int_{-\infty}^{\infty} -\left[C_0^2\left(\frac{1-d}{\eta} + K\eta\right) - \frac{\eta}{2}A_0 C_0 \xi\right] \mathrm{d}\xi \\ &= -2\sqrt{1 - \frac{\eta^2}{4}}\left[\frac{2}{3}\left(\frac{1-d}{\eta} + K\eta\right)\left(1 - \frac{\eta^2}{4}\right) + \frac{\eta}{2}\right]. \end{aligned}$$

The function $\Delta(0, \eta)$ measures the distance between $P(\Gamma_+)$ and $P^{-1}(\Gamma_-)$ to $\mathcal{O}(a)$. Applying the Implicit Function Theorem, a simple zero η_i of $\Delta(0, \eta)$ defines a transversal intersection point of $P(\Gamma_+)$ and $P^{-1}(\Gamma_-)$ at $B = 0$.

We analyse the zeros of the Melnikov function. Setting $\Delta(0, \eta) = 0$ leads to

$$\eta = 2 \quad \text{or} \quad K\eta^4 - (4K + d + 2)\eta^2 + 4(d - 1) = 0.$$

However, since Δ is not defined at $\eta = 2$, solutions of the fourth-order equation are the only possible candidates for a zero of the Melnikov function. Note that solutions have to be positive and satisfy $0 < \eta_{\min} < \eta < \eta_{\max} < 2$. The solutions of this equation are given by the positive solutions of

$$\eta^2 = \kappa_\pm = \frac{1}{2K}\left(4K + d + 2 \pm \sqrt{(4K + d + 2)^2 - 16K(d - 1)}\right).$$

For $d < 4$, the expression under the square root is positive, leading to two possible (positive) solutions. When $d > 2$, we find that $\kappa_+ < 0$ for $K < 0$ and $\kappa_+ > 4$ for $K > 0$, and the extra restriction $0 < \eta < 2$ can only be satisfied by $\eta_- = \sqrt{\kappa_-}$.

Further analysis shows that $0 < \kappa_- < 4$ is satisfied for all K. Moreover, κ_- is not defined for $K = 0$ and to leading order $\kappa_- = \frac{d-1}{K} \to 0$ as $K \to \infty$ and $\kappa_- = 4 + \frac{3}{K} \to 4$ as $K \to -\infty$ to leading order. Using these asymptotic expansions, we find restrictions on K since the zero η_- needs to lie between $\eta_{\min} = ak_b \log \frac{1}{a}$ and $\eta_{\max} = 2 - \sqrt{a}$. This gives the leading order restriction

$$-\frac{3}{4\sqrt{a}} < K < \frac{d-1}{\eta_{\min}^2}. \tag{5.9}$$

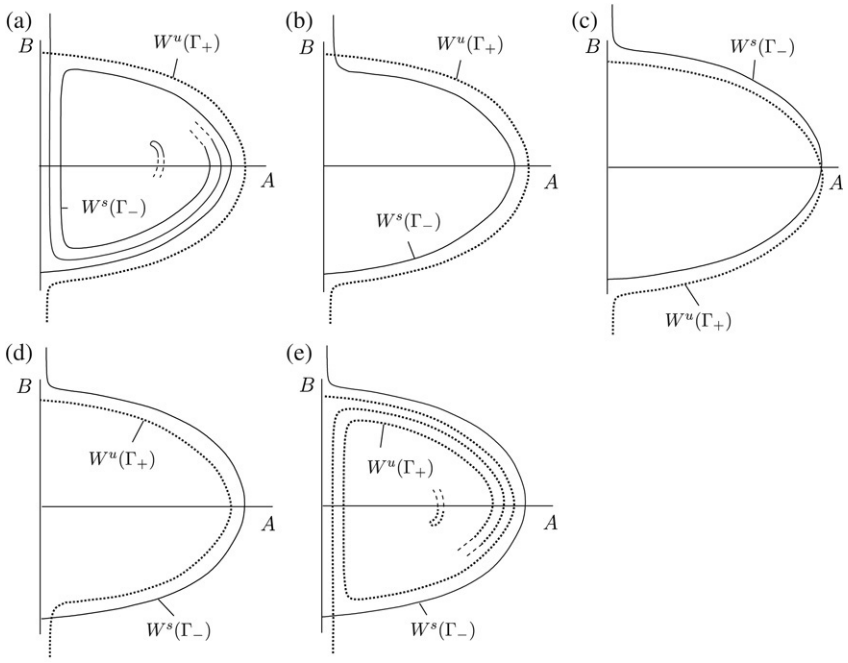

Fig. 6. A sequence of sketches of the manifolds $W^u(\Gamma_+)$ (dotted curve) and $W^s(\Gamma_-)$ (solid curve) in the A–B plane as η increases from $\eta_{\min}$ to $\eta_{\max}$. Their positions are determined in Section 5. (a) At $\eta = \eta_{\min}$, $W^s(\Gamma_-)$ is curled up inside $W^u(\Gamma_+)$ and starts to pull back as η increases. As long as $\eta_{\min} \leq \eta < \eta_{\text{zero}}$, $W^u(\Gamma_+)$ lies 'outside' $W^s(\Gamma_-)$ at $B = 0$. (b) The smaller the value of a, the more the tongue winds around the centre point, and hence in the sketch we only show the tip of the tongue and not all the spirals. (c) For $\eta = \eta_{\text{zero}}$, the two manifolds intersect at $B = 0$. Increasing η further (d), $W^u(\Gamma_+)$ starts to curl up inside $W^s(\Gamma_-)$ up to $\eta_{\max}$ (e) where for $\eta_{\text{zero}} \leq \eta < \eta_{\max}$, $W^u(\Gamma_+)$ lies 'inside' $W^s(\Gamma_-)$ at $B = 0$.

However, this property always holds since K is chosen to be positive and $\frac{1}{a^2(\log\frac{1}{a})^2} \gg 1$, whereas $K = \mathcal{O}(1)$. Thus, the two manifolds intersect transversely in a point that is $\mathcal{O}(a)$ close to $(\sqrt{2(1-\frac{\eta_i^2}{4})}, 0, \eta_i)$ with $\eta_i = \sqrt{\kappa_-}$. We label the η value of the actual intersection point by $\eta = \eta_{\text{zero}}$; see Fig. 6(c).

The adiabatic Melnikov function also gives the orientation of $W^u(\Gamma_+)$ with respect to $W^s(\Gamma_-)$ at $B = 0$. We find that $\Delta(0,\eta) > 0$ for $\eta_{\min} < \eta < \eta_{\text{zero}}$; and, thus, $W^u(\Gamma_+)$ lies 'outside' $W^s(\Gamma_-)$, i.e., $p_1 > p_2$ for points $(p_1, 0, \eta) \in P(\Gamma_+)$ and $(p_2, 0, \eta) \in P^{-1}(\Gamma_-)$; see Fig. 6(a) and (b). Similarly, $\Delta(0,\eta) < 0$ for $\eta_{\text{zero}} < \eta < \eta_{\max}$; and, therefore, $W^u(\Gamma_+)$ lies 'inside' $W^s(\Gamma_-)$, i.e., $p_1 < p_2$ for points $(p_1, 0, \eta) \in P(\Gamma_+)$ and $(p_2, 0, \eta) \in P^{-1}(\Gamma_-)$; see Fig. 6(d) and (e).

5.3. *The locations of segments of $W^u(\Gamma_+)$ and $W^s(\Gamma_-)$ on constant η slices*

In this section, we determine the locations of long segments of the manifolds $W^u(\Gamma_+)$ and $W^s(\Gamma_-)$ on $\eta =$ constant planes for $\eta_{\min} < \eta < \eta_{\max}$; see Fig. 6. Since the results of the previous section are similar to the ones in [21], only the position of the intersection point differs; the analysis of [21] can be adjusted and applied here. This analysis makes use of the fact that the manifolds are smooth, and of the Exchange Lemma [13,14] from geometric singular perturbation theory. We will only state the results here and refer the reader to Section 6 of [21] for details of the analysis.

In summary, we find that the manifolds $W^u(\Gamma_+)$ and $W^s(\Gamma_-)$ behave as in Fig. 6 when η is varied from $\eta_{\min}$ to $\eta_{\max}$. As η increases from the value corresponding to the slice shown in Fig. 6(d) to that corresponding to Fig. 6(e), this segment of $W^u(\Gamma_+)$ curls up inside $W^s(\Gamma_-)$ in a tongue-like way; see Fig. 6(e).

Moreover, there is a segment of $W^s(\Gamma_-)$ that curls up inside $W^u(\Gamma_+)$ for $\eta_{\min} < \eta < \eta_{\text{zero}}$ in a tongue-like way; see Fig. 6(a). At $\eta = \eta_{\min}$, $W^s(\Gamma_-)$ is curled up the most, and as η is increased the tongue that is formed by $W^s(\Gamma_-)$ inside $W^u(\Gamma_+)$ starts to retract. This continues up to $\eta = \eta_{\text{zero}}$, where the manifolds intersect at the B-axis; see Fig. 6(c).

The extent to which $W^u(\Gamma_+)$ and $W^s(\Gamma_-)$ curl up inside themselves depends on the magnitude of a. A smaller value of a results in longer tongue structures of $W^s(\Gamma_-)$ at $\eta = \eta_{\min}$ and of $W^u(\Gamma_+)$ at $\eta = \eta_{\max}$.

Detailed behaviour of $W^s(\Gamma_-)$ and $W^u(\Gamma_+)$ that is needed in the analysis in Section 6 also can be concluded. Near $\eta_{\max}$, the segment of $W^u(\Gamma_+)$ which is parallel to the B-axis and closest to it lies exponentially close to the B-axis. There, the width of the tongue is $\mathcal{O}(a)$. And hence, the right boundary of the tongue is $\mathcal{O}(a)$ away from the B-axis. Moreover, the segment of $W^s(\Gamma_-)$ that lies closest to the B-axis, and that forms the left boundary of the tongue there, is exponentially close to the B-axis at $\eta = \eta_{\min}$. Finally, the right boundary of the tongue there is $\mathcal{O}(a)$ away from the B-axis.

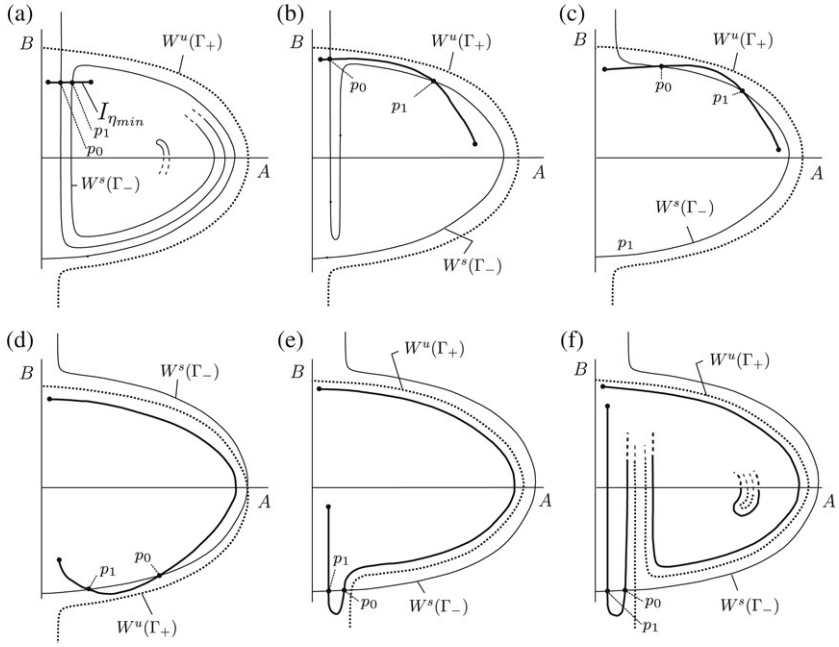

Fig. 7. The transformation of I_η as η is increased from $\eta_{\min}$ to $\eta_{\max}$. During this process the point p_0 remains on $W^u(\Gamma_+)$, and the point p_1 remains on $W^s(\Gamma_-)$. (a) At $\eta = \eta_{\min}$, I_η is an interval approximately perpendicular to the B-axis. The smaller the value of a, the more the tongue winds around the centre point, and hence in the sketch we only denote the tip of the tongue and not all the spirals. ((b)–(d)) A–B planes at different values of η in Step I. I_η curls up as $W^u(\Gamma_+)$ pulls back, where frame (d) is a sketch for $\eta = \eta_{\text{zero}}$. ((e), (f)) In step II, $W^u(\Gamma_+)$ curls up in itself like a tongue. (f) At $\eta = \eta_{\max}$, I_η has formed a tongue structure as a result of the fact that $W^u(\Gamma_+)$ curls up.

6. Tracking M_0 from ξ_b to $\xi_{\max}$ (i.e., from $\eta_{\min}$ to $\eta_{\max}$) and the intersections of M^0 and M^∞ at $\eta_{\max}$

In this section, we track the manifold M_0 from $\eta_{\min}$ to $\eta_{\max}$. It will be useful to define $\eta =$ constant slices of M_0. Following [21] we denote these by I_η. The location of $I_{\eta_{\min}}$ was already determined in Section 4; $I_{\eta_{\min}}$ is a nearly horizontal line segment that stretches out over the interval $(0, ca^m]$ in the A coordinate and with $B = 1$ to leading order, as was first shown in Fig. 4 and as is shown again here – now with the manifolds – in Fig. 7(a).

In order to show that $I_{\eta_{\min}}$ does indeed intersect with $W^s(\Gamma_-)$ as shown in Fig. 7(a), we first recall from Lemma 4.4 that on $I_{\eta_{\min}}$: $B < 1 - \frac{d-1}{2k_2 \log \frac{1}{a}}$ for some constant $k_2 > 0$. Secondly, we determine the value of B at the intersection point of $W^u(\Gamma_+)$ with the B-axis. For $\eta = \eta_{\min} = ak_b \log \frac{1}{a}$, this value of B is given by $B = \alpha = \sqrt{1 - \frac{\eta_{\min}^2}{4}} = 1 - \frac{1}{8}a^2k_b^2 \log^2 \frac{1}{a}$ to leading order, using that $\eta_{\min} \ll 1$. Combining this with the fact that the tongues are of $\mathcal{O}(a)$ width (Section 5.3), we conclude that the value of B on $W^s(\Gamma_-)$ close to the upper saddle point is to leading order given by $B = 1 - \frac{1}{8}a^2k_b^2 \log^2 \frac{1}{a} - ca = 1 - ca$. This value of B is larger than the maximum value of B on $I_{\eta_{\min}}$ (which is $B = 1 - \frac{d-1}{2k_2 \log \frac{1}{a}}$) so that the position of $I_{\eta_{\min}}$ with respect to $W^s(\Gamma_-)$ is indeed as indicated in Fig. 7(a).

Moreover, combining the fact that the A coordinate of $I_{\eta_{\min}}$ stretches out over the interval $(0, ca^m]$ (it also contains exponentially small terms), see Remark 4.1, with the fact that the tongue has $\mathcal{O}(a)$ width, we find that $I_{\eta_{\min}}$ intersects $W^s(\Gamma_-)$ at least in the points p_0 and p_1 as shown in Fig. 7(a).

The points on I_η must respect the invariance properties of the manifolds $W^u(\Gamma_+)$ and $W^s(\Gamma_-)$. First, points on I_η that are also on the manifold $W^s(\Gamma_-)$, e.g., the points p_0 and p_1 in Fig. 7(a), must remain on $W^s(\Gamma_-)$ for as long as it exists. And, orbits that do not start on either $W^u(\Gamma_+)$ or $W^s(\Gamma_-)$ will never intersect these manifolds. Also, if we choose the left end point of $I_{\eta_{\min}}$ sufficiently close to the B-axis, it will remain close to the B-axis when increasing η from $\eta_{\min}$ to $\eta_{\max}$ since it takes $\mathcal{O}(\frac{1}{a})$ time to pass along the saddle point.

We distinguish two steps in pulling I_η forward; step I from $\eta_{\min}$ to η_{zero} and step II from η_{zero} to $\eta_{\max}$. In step I, the tongue structure of the manifold $W^s(\Gamma_-)$ retracts as illustrated in Fig. 6(a)–(c). As a result I_η becomes a curve that rolls up inside itself (Fig. 7(d)) during this step.

In step II, $W^u(\Gamma_+)$ starts to curl up into itself like a tongue, as illustrated in Fig. 6(e). Since the positions of all the points on I_η with respect to $W^u(\Gamma_+)$ and $W^s(\Gamma_-)$ have to remain the same, I_η will also start to curl up into itself like a tongue; see Fig. 7(f). The curve $I_{\eta_{\max}}$ has the important properties that there are segments that are C^1 exponentially close to the B-axis (namely segments containing the type L intersection points — one segment for each such point), and that there are other segments that are C^1 close to

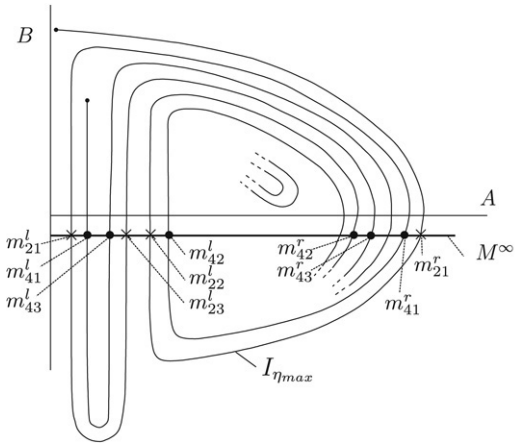

Fig. 8. A sketch of M^∞ and I_η at $\eta = \eta_{\max}$ in the A–B plane. At the points marked by a cross, the m^r_{21} and m^l_{2i}, $k = 2$ solutions are formed for $i = 1, 2, 3$. At the points marked by a dot, the m^r_{4i} and m^l_{4j}, $k = 4$ solutions occur for $i, j = 1, 2, 3$. The existence of all of these intersection points is demonstrated in Section 6. Note that only some of the intersection points that form a $k = 4$ solution are sketched here, to maintain clarity in this figure.

$W^u(\Gamma_+)$ (namely one segment for each of – and containing – the intersection points of type R); see Fig. 8. Hence, the intersections of $I_{\eta_{\max}}$ with M^∞ are all transverse.

The structure as sketched in Fig. 8 is more complicated than the sketch of $I_{\eta_{\max}}$ given in Fig. 7(f). When constructing Fig. 8, we took into account that both $W^s(\Gamma_-)$ at $\eta_{\min}$ and $W^u(\Gamma_+)$ at $\eta_{\max}$, for smaller values of a, wind around in the (A, B)-plane more than is sketched in Fig. 7(a) and (f). The fact that at $\eta_{\min}$, $W^s(\Gamma_-)$ has made more excursions around the centre point implies that there exist more intersection points of $W^s(\Gamma_-)$ and $I_{\eta_{\min}}$ than are given in Fig. 7(a) (and leads to a different location of one of the end-points of the curve). Then, carefully tracking I_η as η increases from $\eta_{\min}$ and also taking into account that $W^u(\Gamma_+)$ winds around the centre point more than is sketched in Fig. 7(f) leads to the sketch in Fig. 8.

On M^0 at $\xi_{\max}$ we have the following estimates of B and A, where we denote these values by $B^0(\xi_{\max})$ and $A^0(\xi_{\max})$:

Lemma 6.1. *For points on the curve I_η at $\xi = \xi_{\max}$, the values of $B^0(\xi_{\max})$ are mapped onto the interval $(-a^{\frac{1}{4}} + \frac{1}{8}a^{\frac{3}{4}}, a^{\frac{1}{4}} - \frac{1}{8}a^{\frac{3}{4}})$.*

The proof of this lemma uses the fact that the solutions lie $\mathcal{O}(a)$ close to the heteroclinic orbit (5.4) of the unperturbed system where its B value varies between $-\sqrt{1 - \frac{\eta^2_{\max}}{4}}$ and $\sqrt{1 - \frac{\eta^2_{\max}}{4}} = a^{\frac{1}{4}}\sqrt{1 - \frac{1}{4}\sqrt{a}} = a^{\frac{1}{4}} - \frac{1}{8}a^{\frac{3}{4}} + hot$. See the proof of Lemma 7.1 in [21] for details.

Combining this result with the estimate obtained in Lemma 3.2, stating $B^\infty_d(\xi_{\max}) = -a^{\frac{1}{4}} + c_1\sqrt{a}$, one finds that there are solutions on M^0 and M^∞ such that the B coordinates of these solutions overlap at $\xi_{\max}$.

We also have the following estimate for $A^0(\xi_{\max})$:

Lemma 6.2. *The intersection points of the curve I_η and the line $B^\infty_d(\xi_{\max}) = -a^{\frac{1}{4}} + c_1\sqrt{a}$ can be split into two groups. One group of points lies close to the heteroclinic orbit (5.4) of the unperturbed problem, (2.12) with $a = 0$ and $\eta = \eta_{\max}$. For these points, $A^0(\xi_{\max}) = 2\sqrt{c_1}a^{\frac{3}{8}} - \frac{c_1^2 + \frac{1}{4}}{2\sqrt{c_1}}a^{\frac{5}{8}} + hot$, and we label these as points of type R. For the other intersection points, $A^0(\xi_{\max})$ is exponentially small, and we label them as points of type L. Hence, the A coordinates of all intersection points lie in the interval $(0, 2\sqrt{c_1}a^{\frac{3}{8}})$.*

In the proof of this lemma it is again used that solutions of type R lie close to the heteroclinic orbit (5.4) of the unperturbed problem, (2.12) with $a = 0$ and $\eta = \eta_{\max}$. Details of the proof can be found in the proof of Lemma 7.2 in [21].

Hence, there are solutions on M^0 and M^∞ for which the A coordinates coincide at $\eta_{\max}$, since we showed in Lemma 3.4 that $A^\infty_d(\xi_{\max})$ is onto $(0, a^{\frac{3}{8}}]$ (including the exponentially small terms) as a function of $A_1 = A(\frac{\sqrt{2}}{a\sqrt{a}})$.

Therefore, we find that there are solutions on M^0 and M^∞ for which the A and B coordinates at $\xi_{\max}$ are the same. Moreover, the manifolds M^0 and M^∞ intersect transversely in the A–B plane at $\xi = \xi_{\max}$.

The above results are almost enough to prove Theorem 2.1. There are three outstanding issues. First, we need to show that the assumption on ϕ that we made above, namely that $|\phi| < a^{\frac{1}{2}}$ for $\xi \leq \xi_{\max}$, is satisfied. This is proven in Section 7. Second, we need to extract some more quantitative information about the full solutions that lie in the transverse intersections of M^0 and M^∞, such as locations of local maxima and distances between them, as stated in the theorem. This is done in Section 8. Third, while solutions can be chosen so that the A and B coordinates are the same at $\xi = \xi_{\max}$, it is not necessarily the case that the ψ coordinates of these solutions also agree. Therefore, in Section 9, we analyse the dynamics of the ψ coordinate. We show that for each of the distinct intersection points found above there is a locally unique d such that the ψ coordinates also coincide. That completes the

proof of the desired result that the three-dimensional manifolds M^0 and M^∞ have two families of transverse intersection points in the A–B–ψ–ξ–d, extended, five-dimensional phase space and, hence, that the locally unique, multi-bump solutions claimed in Theorem 2.1 exist, with the properties stated there.

Remark 6.1. As was already noted in Remark 3.1, we can use a more general setting and pull back M^∞ to a point $\xi = \frac{2-b}{a}$ where $a^{\frac{2}{3}} \ll b \ll a^{\frac{2}{5}}$. This can be done as follows: at $\eta = 2-b$, the constant η slice of M_0 lies exponentially close to the heteroclinic orbit that exists for $a = 0$. Thus, to make sure that M^0 and M^∞ intersect, we must have that the projection of M^∞ at $\xi = \xi_{\max}$ lies within this heteroclinic orbit. This is satisfied when $B_d^\infty(\xi_{\max}) \gg -\sqrt{1-\frac{\eta_{\max}^2}{4}}$ and this leads to the condition $b \ll a^{\frac{2}{5}}$. The $a^{\frac{2}{3}}$-boundary is needed to insure that the higher order terms in $B(\eta = 2-b)$ are really of higher order. A different choice of $\eta_{\max}$ would of course also influence other estimates, for example Lemma 6.2 concerning the estimates of A at $\xi = \xi_{\max}$ in the multi-bump region.

7. The bound on ϕ

In the foregoing tracking analysis, we assumed that $|\phi| < a^{\frac{1}{2}}$ for $\xi \le \xi_{\max}$ so that system (2.12) indeed contains the leading order terms of (2.9). We now turn to proving this statement. The explicit expression (4.3) for ϕ obtained in Lemma 4.2 enables us to approximate ϕ for $\xi \le \xi_{\max}$ as follows:

Lemma 7.1. *For the values of d, K, b such that there exist constants $c > 0$ and $l > \frac{1}{2}$ with*

$$\frac{1}{A^2(\xi_b)}\left|\int_{\xi_b}^{\xi} A^2(y)\left[\frac{d-2+2K}{2} - K(b+1)A^2(y) - \frac{Ka^2y^2}{2}\right]\mathrm{d}y\right| \le ca^{-\frac{3}{4}+l} \tag{7.1}$$

for every $\xi_b < \xi < \xi_{\max}$, there exists a positive constant c_1 such that

$$|\phi(\xi)| \le c_1 a^{l_1} < c_1 a^{\frac{1}{2}},$$

where $l_1 = \min(\frac{5}{8}, l)$

The proof of this lemma is given in Appendix D, and is based on continuous induction.

Now, we can finally choose the value of k_b. In Remark 4.1 and the proof of Lemma 7.1 we made the following assumptions on the relation between k_b and m_r:

$$\frac{3}{8} < m = m_r - k_b < 1.$$

In the remaining part of this article we do not need to assume anything else for k_b; therefore, we choose k_b and m_r such that the above holds.

In Lemma 7.1, we assumed that the coefficients d, a, K and b satisfy the restriction (7.1) where the solution still occurs in the expression. Here, we analyse restriction (7.1) and study which relation between d, a, K and b has to be satisfied in order for (7.1) to hold. We determine bounds of the integrals to obtain a relation between the coefficients which leads to

Lemma 7.2. *Assumption (7.1) in Lemma 7.1 holds as long as there exist constants $c_1, c_2, c, \tilde{c} > 0$, c_3, and $l > \frac{1}{2}$ such that*

$$|c_1(d-2) - c_2K + c_3b| \le ca^{-\frac{3}{4}+l}\mathrm{e}^{-\frac{\tilde{c}}{a}}. \tag{7.2}$$

For $b = 0$ in the case of the $k = 2$ solution, the above relation reduces to

$$\left|\frac{d-2}{2} - \frac{5}{3}K\right| + \frac{8\sqrt{2}}{9\sqrt{3}}K \le ca^{-\frac{3}{4}+l}\mathrm{e}^{-\frac{\tilde{c}}{a}}. \tag{7.3}$$

The proof of this lemma is given in Appendix E. We use the fact that the solutions lie close to the heteroclinic orbit, in order to bound the integral in (7.1).

Remark 7.1. It is noted in the proof of this lemma that several, but not all, of the solutions of Theorem 2.1 still exist in the case where relation (7.2) does not hold, but when instead

$$|c_1(d-2) - c_2K + c_3b| \le ca^{l_1}, \tag{7.4}$$

where $l_1 = \min\{\frac{3}{4}, -\frac{3}{4} + l + 2m_b\}$ and $A(\xi_b) = c_b a^{m_b}$, is satisfied. Solutions for which $A(\xi_b)$, and hence $A(0)$, is exponentially small can no longer be constructed but the other solutions for which $A(\xi_b) = c_b a^{m_b}$ can. Careful study of the construction of I_η at $\eta = \eta_{\max}$ implies that the solutions corresponding to the intersection points $m_{21}^r, m_{22}^l, m_{23}^l, m_{42}^r, m_{43}^r$ and the solutions with $k \ge 6$

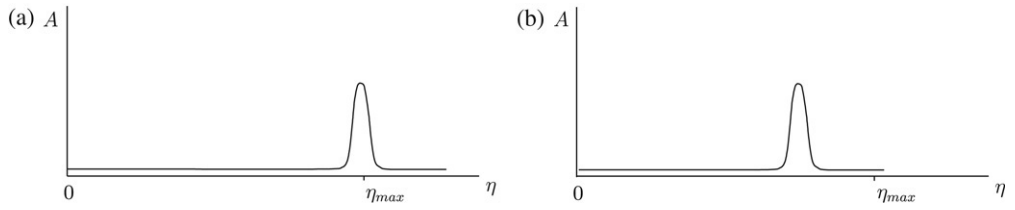

Fig. 9. A sketch of the different types of $k = 2$ solutions. (a) The solution of type R created at m^r_{21}. (b) The three solutions of type L, which are exponentially close to each other and hence indistinguishable in this sketch, correspond to the three intersection points m^l_{2i}, $i = 1, 2, 3$.

(k even) that are formed from these solutions no longer exist. However, the other solutions still do. Hence, on changing condition (7.2)–(7.4) only some of the solutions in Theorem 2.1 can be constructed. Although not all of the solutions in the theorem are found, for every even k, there do still exist solutions with k maxima.

8. The intersections of M^0 and M^∞ and the multi-bump solutions

In Lemma 6.2, we showed that the intersection points of M^0 and M^∞ can be split into two types, L and R. We labelled the intersection points m^l_{ij} and m^r_{ij}, where $i, j \in \mathbf{N}$, corresponding to points of type L and R, respectively, with the superscript corresponding to the type of the intersection point and with the index i denoting the number of maxima of the solution on the real line.

The number of maxima of a solution is determined by the number of times I_η winds around the centre point in the A–B plane as η increases from $\eta_{\min}$ to $\eta_{\max}$. Each time that I_η crosses the A-axis close to the heteroclinic orbit, an extra maximum is added. Thus, by carefully keeping track of the number of these crossings, one can determine the number of maxima of a solution corresponding to an intersection point. A $k = n$ solution consists of n maxima on the whole real line, and hence $\frac{n}{2}$ maxima for $\xi > 0$; the values of η where these maxima occur are all smaller than $\eta_{\max}$.

8.1. The $k = 2$ solutions

We will start by describing the $k = 2$ solutions that correspond to the four intersection points labelled $m^r_{21}, m^l_{21}, m^l_{22}, m^l_{23}$ in Fig. 8. We do this by keeping track of I_η as η increases from $\eta_{\min}$ to $\eta_{\max}$.

There is a qualitative difference between the solution that is constructed at m^r_{21} and the ones at the points m^l_{2i}. This difference comes from the type, R or L, of the solution, i.e., the value of $A(\eta_{\max})$ differs at the intersection of M^0 and M^∞. Therefore, the maximum of the solution will be reached at a different value of η for the two different types of solutions. The maximum of the $k = 2$ solution corresponding to m^r_{21} is reached for η close to $\eta_{\max}$; and at this maximum $A_{\max} = \sqrt{2(1 - \frac{\eta^2_{\max}}{4})} = \sqrt{2}a^{\frac{1}{4}}(1 - \frac{1}{8}\sqrt{a})$ to leading order. Thus, the value of A at the maximum is given by $A = A_{\max} + c_2 a$ for some constant c_2; see Fig. 9(a) for a sketch of this 2-bump. For the 2-bumps corresponding to the points m^l_{2i}, $i = 1, 2, 3$, the value of A at $\eta_{\max}$ is exponentially small. Thus, the second maximum is reached well before $\eta = \eta_{\max}$; see Fig. 9(b). Moreover, the points m^l_{2i} all lie exponentially close to each other for $\eta > \eta_{\text{zero}}$; and, therefore, the three solutions of type L lie exponentially close to each other.

8.2. The construction of $k = n$ solutions for $k = 2$ even and $n \geq 4$

Following the method used above to construct the $k = 2$ solutions, we now show that there exist solutions with n local maxima on the real line for each $n \geq 4$ and n even. The number of $k = n$ solutions can be determined explicitly (for a sufficiently small), where again a qualitative difference occurs between solutions of type R and of type L, as stated in Theorem 2.1.

We continue the argument given in the previous section for $k = 2$ for more general n (n even), starting with $n = 4$, by again studying the intersection of M^0 and M^∞ at $\eta_{\max}$ (for a sufficiently small). As a decreases, the stable and unstable manifolds $W^u(\Gamma_+)$ and $W^s(\Gamma_-)$ curl up more into themselves which implies that I_η also curls up more into itself. More precisely, comparing $W^s(\Gamma_-)$ for $a = a_0$ to $a = a_1$ where $0 < a_1 < a_0 \ll 1$, it is curled up more at $\eta = \eta_{\min}$ for a_1 than for a_0. A similar statement holds for $W^u(\Gamma_+)$ at $\eta = \eta_{\max}$. Therefore, when we follow I_η as η increases from $\eta_{\min}$ to $\eta_{\max}$ we find, using the two steps distinguished in Section 6, that there exist more intersection points of M^0 and M^∞ at $\eta_{\max}$ besides the points leading to $k = 2$; see Fig. 8. Also, the number of times that one crosses the A-axis near $A_{\max}$ to reach such an intersection point increases, and therefore, the number of maxima of a solution increases. Note that one extra crossing near $A_{\max}$ in this construction leads to one extra maximum for $\xi > 0$, and hence, to two extra maxima on the real line (solutions are symmetric).

First, we focus on the $k = 4$ solutions that are formed in a similar way as the $k = 2$ solutions. In step I of the transformation of I_η, as it winds around the A–B plane, a segment of I_η has intersected with the A-axis twice at $A_{\max}$, which results in the construction of $k = 4$ solutions at the points m^r_{41} and m^l_{41}; see Fig. 8. In step II where I_η forms a tongue, this same part of I_η will again intersect with M^∞, this time exponentially close to 0. These intersection points, m^l_{42} and m^l_{43} (see Fig. 8), correspond to a pair of $k = 4$

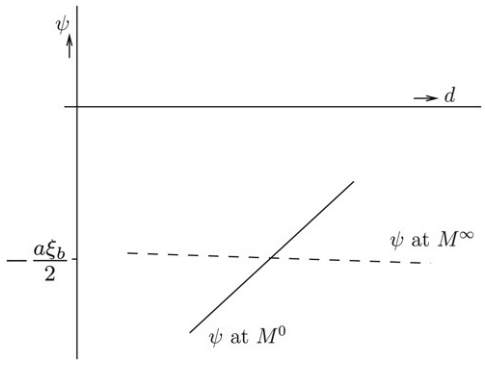

Fig. 10. A sketch of the ψ coordinates of the manifolds M^0 (solid curve) and M^∞ (dashed curve) at $\xi = \xi_{\max}$ as a function of d.

solutions of type L. So far, the solutions are all constructed in a similar way as the $k = 2$ solutions. However, more $k = 4$ solutions are formed in step II. These are constructed from the tongue-like branch on which the points m^l_{22} and m^l_{23} lie. This branch winds around the A–B plane to intersect once again with the A-axis close to $A_{\max}$ and, therefore, when it intersects with M^∞ at m^r_{42} and m^r_{43} two extra $k = 4$ solutions of type R are formed. These solutions have an extra maximum for $\xi > 0$ compared to the solutions at the points m^l_{22} and m^l_{23} and therefore form $k = 4$ solutions. As I_η curls up further (for a sufficiently small), this branch will again intersect with M^∞ exponentially close to $A = 0$ to give two extra $k = 4$ solutions of type L; these are not shown in Fig. 8. Thus, for a sufficiently small, there exist eight $k = 4$ solutions, three of which are of type R and five are of type L. Finally, the points m^l_{4i} all lie exponentially close to each other.

The number of $k = 4$ solutions follows easily from the number of $k = 2$ solutions. One $k = 4$ solution of type R and three $k = 4$ solutions of type L are formed in a similar way to the $k = 2$ solutions. Besides these, two extra $k = 4$ solutions of type R and two of type L are formed on the branches where the $k = 2$ solutions occur. Thus, the number of $k = 4$ solutions of type L increases by 2 with respect to the number of $k = 2$ solutions of type L, and the same holds for the number of $k = 4$ solutions of type R.

Inductively, the $k = n + 2$ solutions can be formed from the $k = n$ solutions, and the number of $n + 2$ solutions also follows from the number of $k = n$ solutions, as long as $n + 2 \leq n_0(a)$ for the given, sufficiently small, value of a. The number of solutions of both types L and R increases by 2 as the number of maxima increases from n to $n + 2$.

9. Matching the ψ coordinate

So far, we have showed that on the cross section $\xi = \xi_{\max}$ there exist two families of solutions on M^0 and M^∞ for which the A and B coordinates are the same (for a sufficiently small). In order to complete the proof of Theorem 2.1, we will show that d can be chosen such that the ψ coordinates of M^0 and M^∞ are the same. The analysis of the ψ coordinate consists of two parts. First, we show that, at $\xi = \xi_{\max}$, the interval of possible values of ψ on M^0 overlaps the interval of possible values on M^∞. In Section 3.1 we showed that the distance between $\psi^\infty_d(\xi_{\max})$ and $\frac{-a\xi_{\max}}{2}$ is $ca^{d-\frac{1}{2}}$; see Lemma 3.2. Therefore, to ensure that the intervals of the possible values of ψ on M^0 and on M^∞ overlap, it is sufficient to show that the distance between $\psi^0_d(\xi_{\max})$ and $\frac{-a\xi_{\max}}{2}$ is larger than $ca^{d-\frac{1}{2}}$, for a range of d values. Secondly, we show that the intersection is transversal so that d can be chosen such that $\psi^\infty_d(\xi_{\max})$ and $\psi^0_d(\xi_{\max})$ match; see Fig. 10.

9.1. Overlap of the ψ-intervals

First, we show that $|\psi^0_d(\xi_{\max}) + \frac{a\xi_{\max}}{2}|$ is larger than $ca^{d-\frac{1}{2}}$. We get a lower bound from the expression (4.3).

Lemma 9.1. *There exists a constant $c > 0$ such that $|\phi^0_d(\xi_{\max})| = |\psi^0_d(\xi_{\max}) + \frac{a\xi_{\max}}{2}| \geq ca^{d-\frac{1}{2}}$.*

A proof of this lemma is given in Appendix F.

This lemma implies that, as we vary d, the interval of values of $\psi^0_d(\xi_{\max})$ overlaps the interval of values of $\psi^\infty_d(\xi_{\max})$.

9.2. The transversal intersection

Here, we show that there exists a locally unique value of d for which $\psi^0_d(\xi_{\max}) = \psi^\infty_d(\xi_{\max})$. Specifically, we prove that the intersection of $\psi^0_d(\xi_{\max})$ and $\psi^\infty_d(\xi_{\max})$ as functions of d is transversal by examining the derivatives of $\psi^\infty_d(\xi_{\max})$ and $\psi^0_d(\xi_{\max})$ with respect to $\Delta = d - 2$.

From Lemma 3.2 we know that $|\psi_d^\infty(\xi_{\max}) + \frac{a\xi_{\max}}{2}| = ca^{d-\frac{1}{2}}$, leading to

$$\frac{\partial \psi_d^\infty(\xi_{\max})}{\partial \Delta} \leq ca^{d-\frac{1}{2}} \log(a) \ll ca^{d-\frac{3}{4}},$$

for some positive constant c. Now, we will show that the derivative of $\psi_d^0(\xi_{\max})$ with respect to Δ is larger than $ca^{d-\frac{3}{4}}$. We do this in two steps. First, we determine an upper bound for the derivative at $\xi = \xi_b$; see Lemma 9.2. We need this upper bound to obtain, in the second step, an estimate of a lower bound of the derivative at $\xi = \xi_{\max}$, Lemma 9.3.

Using expression (4.3), the derivative of ψ with respect to Δ is

$$\frac{\partial \phi(\xi)}{\partial \Delta} = \frac{\partial \psi(\xi)}{\partial \Delta} = \frac{a\xi^{1-d} I}{A^2(1+a^2K^2)}\left(\log \xi^{-1} - \frac{2}{A}\frac{\mathrm{d}A}{\mathrm{d}\Delta}\right) + \frac{a\xi^{1-d}}{A^2(1+a^2K^2)}\frac{\mathrm{d}I}{\mathrm{d}\Delta},$$

where

$$\begin{aligned}\frac{\mathrm{d}I}{\mathrm{d}\Delta} &= \int_0^\xi A^2 y^{d-1} R(y)\left(\log y + \frac{2}{A(y)}\frac{\mathrm{d}A}{\mathrm{d}\Delta}\right)\mathrm{d}y + \int_0^\xi A^2 y^{d-1} S(y) \\ &= I_1 + I_2\end{aligned}$$

and

$$S(y) = \frac{1}{2} - 2K(b+1)A\frac{\mathrm{d}A}{\mathrm{d}\Delta} + Kay\frac{\mathrm{d}\phi}{\mathrm{d}\Delta} + k_1\left(1 - (b+1)A^2 + ay\left(\phi - \frac{ay}{2}\right)\right)$$

with $K = k_1(d-2)$ and where $R(y)$ is as defined in Lemma 4.2.

Remark 9.1. It is unknown whether the constant K depends on d but we do expect and assume this here. A relation between the parameters does follow in the asymptotic construction in [6] and the assumption (2.2), and therefore, we assume that there is a dependence. In the case where there is no relation, the expression for $\frac{\partial \psi(\xi)}{\partial \Delta}$ simplifies with setting $k_1 = 0$.

First, we obtain an upper bound for $\frac{\partial \psi(\xi)}{\partial \Delta}$ at $\xi = \xi_b$.

Lemma 9.2. *There exists a constant $c_1 > 0$ such that $|\frac{\partial \phi(\xi)}{\partial \Delta}| = |\frac{\partial \psi_d^0(\xi)}{\partial \Delta}| \leq c_1 a^{\frac{3}{4}}$ for every $0 < \xi < \xi_b$.*

The proof of this lemma follows by bounding the terms in $\frac{\partial \psi_d^0(\xi)}{\partial \Delta}$ separately and is given in Appendix G.

Using the above result, we now obtain a upper bound for $\frac{\partial \psi_d^0(\xi_{\max})}{\partial \Delta}$.

Lemma 9.3. *There exists a constant $c_2 > 0$ such that $|\frac{\partial \phi(\xi_{\max})}{\partial \Delta}| = |\frac{\partial \psi_d^0(\xi_{\max})}{\partial \Delta}| > c_2 a$.*

In order to prove this lemma we derive an expression for $\frac{\partial \psi(\xi)}{\partial \Delta}$ by differentiating the expression for ψ that we obtained in the proof of Lemma 9.1 with respect to Δ. Then, we show that one of the terms in the expression for $\frac{\partial \psi(\xi)}{\partial \Delta}$ is dominant by using the result of Lemma 9.2. The proof is given in Appendix H.

The above lemma implies that $\frac{\partial \psi_d^0(\xi_{\max})}{\partial \Delta} \gg \frac{\partial \psi_d^\infty(\xi_{\max})}{\partial \Delta}$; see Fig. 10. Therefore, the intersection of $\psi_d^0(\xi_{\max})$ and $\psi_d^\infty(\xi_{\max})$ at $\xi = \xi_{\max}$ is transverse, which implies that there exists a unique d such that $\psi_d^0(\xi_{\max}) = \psi_d^\infty(\xi_{\max})$.

Acknowledgements

I thank Tasso Kaper for useful conversations. The work of V.R. has been made possible by a fellowship of the Royal Netherlands Academy of Arts and Sciences and was partially supported by the Dutch Science Organisation (VIDI).

Appendix A. The proof of Lemma 3.3

Here, we will prove Lemma 3.3 using the construction that we explained in Section 3.1. First, assume that $y(\xi)$ is exponentially small for $\xi \geq \xi_2$. Then, we can use an integrating factor in (3.7) and show that $\hat{z}$ and $\hat{\phi}$ stay exponentially small for $\xi \geq \xi_2$.

The first equation of (3.7) can be written as $y_\xi = (\bar{z} + \hat{z})y$. If we assume that $\hat{z}$ is exponentially small, the rate of growth of y, integrated backward from ξ_1, is governed by $\bar{z}$. Then, if $y(\xi_1)$ is chosen sufficiently small, using an integrating factor shows that y stays exponentially small for $\xi \geq \xi_2$. We restrict to those solutions for which $y(\xi_1)$ is such that $y(\xi)$ stays exponentially small for $\xi \geq \xi_2$. Combining the above two statements, we can conclude that the solutions satisfy the first property of the space $\mathcal{V}$.

Next, we focus on property b. Rewrite the $(\hat{z},\hat{\phi})$-system as one equation for the complex scalar $\hat{z}+\mathrm{i}\hat{\phi}$. Again, $\hat{z}+\mathrm{i}\hat{\phi}$ can be estimated by the non-homogeneous term $-\frac{1}{2}a^{-\frac{1}{4}}\xi^{1-d}y^2\frac{1-a^2bK^2+\mathrm{i}aK(1+b)}{1+a^2K^2}$, by using an integrating factor. Upon assuming $|y|<2a^{-\frac{1}{8}}$, we find that $|\hat{z}|<\sqrt{a}$ and $\hat{\phi}<c_2a^{d-\frac{1}{2}}(1+b)$ for $\xi\geq\xi_{\max}$.

Finally, we assume that $|\hat{z}|<\sqrt{a}$. By $y_\xi=(\bar{z}+\hat{z})y$, the rate of expansion of y is governed essentially by estimates on $\bar{z}$. We know that $\bar{z}$ approaches $-a^{\frac{1}{4}}$ over a substantial portion of the interval $\xi_{\max}\leq\xi\leq\xi_2$. Therefore, we can choose a subinterval of the parameter range for $y(\xi)$ with $y(\xi_2)$ exponentially small so that, for each $y(\xi_1)$ in that interval, we have $y(\xi)<2a^{-\frac{1}{8}}$ for all $\xi\geq\xi_{\max}$. This concludes the proof of the second property of the space, and from this the statement in the lemma follows. □

Appendix B. The proof of Lemma 4.1

First, we study the linear equation for R and then the full nonlinear equation (1.6). Since we are interested in a solution for which R is small, we can study the linearised equation

$$R_{\xi\xi}+\frac{d-1}{\xi}R_\xi-R=0.$$

By setting $z=2\xi$ and $R=w\mathrm{e}^{-\xi}$ this equation can be rewritten as the canonical Kummer equation

$$zw_{zz}+(d-1-z)w_z+\frac{1-d}{2}w=0.$$

For this Kummer equation, there exist two independent solutions and their long time behaviour, corresponding to $\xi\gg1$, and so $z=2\xi\gg1$, is known. For $z\gg1$, the asymptotic expansion of a solution w is to leading order given by a linear combination of $z^{\frac{1-d}{2}}$ and $\mathrm{e}^z z^{\frac{1-d}{2}}$. Hence for $\xi\gg1$, $R_{\mathrm{lin}}(\xi)=\xi^{\frac{1-d}{2}}[a_1\mathrm{e}^{-\xi}+b_1\mathrm{e}^{\xi}]$, for some constants a_1,b_1, is the leading order of a solution of the linearised equation for R. Then, we use that $T=\frac{R_\xi}{R}$ to determine T at $\xi=\xi_b$ which gives us $T_{\mathrm{lin}}(\xi_b)=1+\frac{1-d}{2k\log\frac{1}{a}}$ to leading order. Thus, T at $\xi=\xi_b$ lies close to $1+\frac{1-d}{2k\log\frac{1}{a}}$.

Now, we turn to the full nonlinear system (4.1). From $R_\xi=RT$ it follows, using $T<1$ for all $0<\xi<\xi_b$, that $R(\xi)=R(0)\mathrm{e}^{\int_0^\xi T(y)\mathrm{d}y}\leq R(0)\mathrm{e}^{\xi}$. Then, with $R(0)\in(0,c_ra^{m_r}]$ we find that $R(\xi_b)\leq R(0)a^{-k_b}<c_ra^{m_r-k_b}=c_ra^m$. Moreover, when $R(0)$ is exponentially small, at $\xi=\xi_b$, R is still exponentially small.

Since R and T are both positive, $R_\xi>0$; hence, R increases for $0<\xi<\xi_b$. Also, the leading order approximation from the linear system gives that $1-\frac{d-1}{2k_3\log(\frac{1}{a})}<T(\xi_b)<1-\frac{d-1}{2k_4\log(\frac{1}{a})}<1$ with $0<k_3<k_4$.

For finite time, T increases. Finally, at $\xi=\xi_b$,

$$\begin{aligned}T_\xi&=\frac{1-d}{\xi_b}T(\xi_b)-T^2(\xi_b)-R^2(\xi_b)+1\\&>\frac{1-d}{\xi_b}\left(1-\frac{d-1}{2k_4\log\frac{1}{a}}\right)-\left(1-\frac{d-1}{2k_4\log\frac{1}{a}}\right)^2-c_r^2a^{2m}+1\\&=\frac{(d-1)(k_b-k_4)}{k_bk_4\log\frac{1}{a}}+\frac{(d-1)^2(2k_4-k_b)}{4k_bk_4^2\left(\log\frac{1}{a}\right)^2}-c_r^2a^{2m}>0\end{aligned}$$

upon assuming that $k_4<k_b$ and $m>0$ since $(\log\frac{1}{a})^{-1}\gg a^{p_1}$ for every $p_1>0$. □

Appendix C. The proof of Lemma 4.2

We define

$$M(y)=A^2(y)y\left(\psi(y)+\frac{ay}{2}\right).$$

Then

$$\begin{aligned}\frac{\mathrm{d}}{\mathrm{d}y}(y^{d-2}M)&=y^{d-2}\left[(d-2)A^2\left(\psi+\frac{ay}{2}\right)+2yAA_y\left(\psi+\frac{ay}{2}\right)+yA^2\left(\psi_x+\frac{a}{2}\right)+A^2\left(\psi+\frac{ay}{2}\right)\right]\\&=\frac{aA^2(y)y^{d-1}}{1+\varepsilon^2}\left[\frac{d-2}{2}+K+\frac{a^2K^2d}{2}-K(b+1)A^2(y)+aKy\psi+a^2K^2yB(y)\right].\end{aligned}$$

For the second equality the equations for A_y and ψ_y in system (2.9) were used. Integrating from 0 to x and substituting M gives the first part of the lemma after using that $\psi = \phi - \frac{ay}{2}$ and $\varepsilon = Ka$. The second expression in the lemma is obtained by integrating the last term in the integral by parts. This can be done since $A_\xi = AB$. □

C.1. *The proof of* Lemma 4.5

We want to show that u is small at ξ_b; the value of v is not relevant, but is needed in the estimate for u. We will make an assumption on a bound of v and show that it is satisfied for all $\tau \le \xi \le \xi_b$. The initial conditions are given by $\hat{B}(0) = 0$, $\hat{\phi}(0) = 0$, and therefore, $\frac{\hat{\phi}_\xi}{\hat{A}_\xi} = 0$ at $\xi = 0$; hence, it follows that $\lim_{\xi\to 0} v(\xi) = 0$. This implies that there is a finite $K > 0$ such that $|v(\tau)| < K$. We assume that $|v| < 2K$ and show that it is satisfied for $\tau \le \xi \le \xi_b$.

In a similar way to in the proof of Lemma 4.4 we approximate $(\hat{A}, \hat{B})$ by $(\hat{R}, \hat{T})$. The equation obtained for $\frac{\hat{T}}{\hat{R}}$ is analogous to the first equation in (4.4) after setting $\phi = 0$ and $a = 0$. System (4.1) gives that $\frac{\hat{T}}{\hat{R}}$ can be made arbitrary small by taking τ large enough. From this it follows by using the facts that $|\phi| < Ca^p$, for some $0 < p < 1$, a small, and $|v| < 2K$, that for τ large enough $|u| < c$ holds at $\xi = \tau$ for any fixed c.

On the trajectories we are following we have $0 < A < \tilde{c}a^m$ so that $|2Au| < \tilde{c}a^m$, and $|2u| < 1$. We will use these properties to estimate $u(\xi_b)$. Integrating the first equation of (4.4) from τ to ξ_b ($\tau < \xi_b$) and using an integrating factor gives

$$u(\xi_b) = u(\tau)\exp\left[\int_\tau^{\xi_b} \Gamma \mathrm{d}u\right] + \int_\tau^{\xi_b} \exp\left[\int_x^{\xi_b} \Gamma \mathrm{d}u\right]\left[\left(2\phi - \frac{a^3xK^2}{1+a^2K^2}\right)v - 2\frac{1-a^2bK^2}{1+a^2K^2}A\right]\mathrm{d}x,$$

where $\Gamma(x) = \frac{1-d}{x} - 3B - Au + \frac{a^2xK}{1+a^2K^2}$. To estimate Γ, we use that $\frac{1-d}{x} < 0$, $|Au| < ca^m$, $\frac{a^2xK}{1+a^2K^2} < \tilde{c}a$ and the fact that τ can be chosen such that $B(\xi) > \frac{1}{2}$ for every $\tau \le \xi \le \xi_b$. This yields $\Gamma < -1$ for every $\tau \le \xi \le \xi_b$, which implies that $\exp[\int_x^{\xi_b} \Gamma \mathrm{d}u] < \exp[-(\xi_b - x)]$. Hence,

$$\begin{aligned}
|u(\xi_b)| &< |u(\tau)|\exp[-(\xi_b - \tau)] + \int_\tau^{\xi_b} \exp[-(\xi_b - x)]\left[\left(2|\phi| + \frac{a^3xK^2}{1+a^2K^2}\right)|v| + 2\frac{1-a^2bK^2}{1+a^2K^2}A\right]\mathrm{d}x \\
&< C\mathrm{e}^{-\xi_b} + \int_\tau^{\xi_b} \exp[-(\xi_b - x)]\left[ca^p + \tilde{c}a^m\right]\mathrm{d}x \\
&= C\mathrm{e}^{-\xi_b} + \left[ca^p + \tilde{c}a^m\right](1 - \mathrm{e}^{\tau-\xi_b}) \\
&< Ca^{k_b} + ca^p + \tilde{c}a^m < \hat{c}a^l,
\end{aligned}$$

for a certain $0 < l < 1$.

So, there exist constants $\hat{c} > 0$ and $0 < l < 1$ such that $u(\xi_b) < ca^l$.

Now we can prove that $|v| < 2K$ holds for all $\tau \le \xi \le \xi_b$ using continuous induction. We integrate the second equation in system (4.4) and apply an integrating factor to obtain

$$\begin{aligned}
|v(\xi_b)| &= \left|v(\tau)\left(1 - 1 + \exp\left[\int_\tau^{\xi_b} \Gamma \mathrm{d}u\right]\right) + \int_\tau^{\xi_b} \exp\left[\int_x^{\xi_b} \Gamma \mathrm{d}u\right]\left[u\left(-2\phi + \frac{a^3xK^2}{1+a^2K^2}\right) - 2a\frac{(1+b)K}{1+a^2K^2}A\right]\mathrm{d}x\right|, \\
&\le |v(\tau)|\left|1 - 1 + \exp\left[\int_\tau^{\xi_b} \Gamma \mathrm{d}u\right]\right| + \int_\tau^{\xi_b} \exp\left[\int_x^{\xi_b} \Gamma \mathrm{d}u\right]\left[|u|\left(2|\phi| + \frac{a^3xK^2}{1+a^2K^2}\right) + 2a\frac{(1+b)K}{1+a^2K^2}A\right]\mathrm{d}x.
\end{aligned}$$

Now, we use that $-1 + \exp[\int_\tau^{\xi_b} \Gamma \mathrm{d}u] < 0$, and that $|u| < ca^l$, $|\phi| < Ca^p$ ($0 < p < 1$), $|A| < c_r a^m$ and $\Gamma(x) < -1$ which yields

$$\begin{aligned}
|v(\xi_b)| &\le |v(\tau)| + \int_\tau^{\xi_b} \mathrm{e}^{-(\xi_b - x)}(C_1a^{l+p} + C_2a^{m+1})\mathrm{d}x, \\
&\le |v(\tau)| + c_1a^{l+p} + c_2a^{m+1}.
\end{aligned}$$

Thus $v(\xi_b)$ remains close to $v(\tau)$ and, since $|v(\tau)| < K$, $|v| < 2K$ holds for all $\tau \le \xi \le \xi_b$. □

Appendix D. The proof of Lemma 7.1

This estimate was already proved in Lemma 4.3 for $\tau < \xi \le \xi_b$. Therefore, we now focus on values of ξ where $\xi_b < \xi \le \xi_{\max}$. We will use the expression (4.3) for ϕ given in Lemma 4.2. First, we bound the integral that we denote by I in (4.3). Assuming that $\xi_b < \xi \le \xi_{\max}$, we can split the integral into two parts, one integrating from 0 up to ξ_b and the other from ξ_b to ξ. For the part containing ϕ, we use continuous induction, similarly to the way it was used in the proof of Lemma 4.3.

By using the estimate in Lemma 4.3, we obtain

$$|I| \leq \left| \int_{\xi_b}^{\xi} A^2(y) y^{d-1} R(y) \mathrm{d}y \right| + C A^2(\xi_b) \xi_b^d.$$

Hence, for $\xi_b < \xi \leq \xi_{\max}$

$$|\phi(\xi)| \leq c_1 a^2 + \frac{a \xi^{1-d}}{A^2(\xi)(1+\varepsilon^2)} \left[\left| \int_{\xi_b}^{\xi} A^2(y) y^{d-1} R(y) \mathrm{d}y \right| + C A^2(\xi_b) \xi_b^d \right].$$

First, we focus on the $\frac{1}{A^2(\xi)}$-term. It follows from $A_\xi = AB$ and the use of an integrating factor that

$$A(\xi) = A(\xi_b) \exp\left[\int_{\xi_b}^{\xi} B \mathrm{d}s \right] \tag{D.1}$$

for every $\xi_b < \xi \leq \xi_{\max}$. In order to determine the integral in the exponent, we use the fact that B lies $\mathcal{O}(a)$ close to the periodic solution $B^{(k)}$ (5.6) of the unperturbed system where $k \to 1$.

First, we determine in more detail how k depends on a. So far, it is only known that $k \to 1$ for the solutions we are studying. Substituting the expressions (5.5) and (5.6) for the periodic solutions $(A^{(k)}(\xi), B^{(k)}(\xi))$ of the unperturbed system into the integral κ_1 (5.7), we obtain

$$\kappa_1 = \alpha^4 \frac{k^2 - 1}{(2 - k^2)^2}. \tag{D.2}$$

The fact that the solution that we constructed lies $\mathcal{O}(a)$ close to the heteroclinic solution then implies that it crosses the A-axis at $(A, B) = (\sqrt{2}\alpha - ca, 0)$ for some positive constant c. Substituting this into expression (5.7) for κ_1 yields

$$\kappa_1 = -\sqrt{2} c a \alpha^3 + \mathcal{O}(a^2). \tag{D.3}$$

Equating the two expressions (D.2) and (D.3) for κ_1 and assuming that k lies close to 1, gives, to leading order,

$$k = 1 - \frac{ca}{\sqrt{2}\alpha},$$

where $c > 0$.

As a next step, we determine the amplitude $A^{(k)}$ at $\xi = -\frac{3}{8} T_0^{(k)}$ for this value of k and assume that it is larger than $A(\xi_b)$. Using the explicit expression for $A^{(k)}$ gives

$$A^{(k)}\left(-\frac{3}{8} T_0^{(k)} \right) = \sqrt{2}\beta \mathrm{dn}\left(-\frac{3}{4} K(k), k \right) = c_1 a^{\frac{3}{8}},$$

to leading order. Choosing $m = m_r - k_b$ in Lemma 4.4 such that $m > \frac{3}{8}$ then implies that $A^{(k)}(-\frac{3}{8} T_0^{(k)}) > A(\xi_b)$. Hence, the solution that we tracked to $\xi = \xi_b$ has not yet reached the point $(A^{(k)}(-\frac{3}{8} T_0^{(k)}), B^{(k)}(-\frac{3}{8} T_0^{(k)}))$.

Now, we study the integral in expression (D.1). Note that integrating the solution from ξ_b up to where it intersects with $B = 0$ for the first time leads to a positive contribution to the integral since B is positive just to the right of ξ_b. We denote the second intersection point of the solution with $B = 0$ by ξ_2. Then, we can bound the integral of B by using the above, combined with the fact that the integration of the periodic solution $B^{(k)}$ over one whole period leads to no contribution in the integral. This yields

$$\int_{\xi_b}^{\xi} B \mathrm{d}s \geq \int_{\xi_b}^{\xi_2} B \mathrm{d}s \geq \int_{-\frac{3}{8} T_0^{(k)}}^{\frac{1}{2} T_0^{(k)}} B^{(k)}(s) \mathrm{d}s + \mathcal{O}(a),$$

where $T_0^{(k)}$ is the period of $B^{(k)}$. This integral can be calculated, since we know an explicit expression (5.6) for $B^{(k)}$. Using relations between the Jacobi elliptic functions, see for example [7], we find that

$$\begin{aligned}
\int_{-\frac{3}{8} T_0^{(k)}}^{\frac{1}{2} T_0^{(k)}} B^{(k)}(s) \mathrm{d}s &= \log\left(\mathrm{dn}\left(\frac{1}{2} T_0^{(k)}, k \right) \right) - \log\left(\mathrm{dn}\left(-\frac{3}{8} T_0^{(k)}, k \right) \right) \\
&= \log\left(\sqrt{1 - k^2} \right) - \log c a^{\frac{3}{8}} \\
&= \frac{1}{2} \log a - \log c a^{\frac{3}{8}} \\
&= \frac{1}{8} \log a + \text{hot}.
\end{aligned}$$

Here, the expression for $T_0^{(k)}$ from Section 5.1 and the expressions for k, and $\alpha = \sqrt{1-\frac{\eta^2}{4}}$, where $\eta \geq \eta_b$, were substituted. Note that this term is negative. Using (D.1), it follows that, to leading order,

$$A(\xi) \geq A(\xi_b)a^{\frac{1}{8}} + \text{hot}$$

for every $\xi_b \leq \xi \leq \xi_{\max}$. Thus, we find that there exists a positive constant c_1 such that

$$\frac{1}{A^2(\xi)} \leq c_1 a^{-\frac{1}{4}} \frac{1}{A^2(\xi_b)} \tag{D.4}$$

for $\xi_b \leq \xi \leq \xi_{\max}$.

Therefore,

$$\begin{aligned}
|\phi(\xi)| &\leq c_1 a^2 + C\frac{a^{\frac{3}{4}}\xi^{1-d}}{A^2(\xi_b)}\left|\int_{\xi_b}^{\xi} A^2(y)y^{d-1}R(y)\mathrm{d}y\right| + C_2 a^{\frac{3}{4}}\xi^{1-d}\xi_b^d \\
&\leq c_1 a^2 + C\frac{a^{\frac{3}{4}}\xi^{1-d}}{A^2(\xi_b)}\left|\int_{\xi_b}^{\xi} A^2(y)y^{d-1}R(y)\mathrm{d}y\right| + C_2 a^{\frac{3}{4}}\xi_b \\
&\leq C\frac{a^{\frac{3}{4}}}{A^2(\xi_b)}\left|\int_{\xi_b}^{\xi} A^2(y)R(y)\mathrm{d}y\right| + C_2 a^{\frac{3}{4}-p_1} \\
&\leq C\frac{a^{\frac{3}{4}}}{A^2(\xi_b)}\left|\int_{\xi_b}^{\xi} A^2(y)\left[\frac{d-2+2K}{2} - K(b+1)A^2(y) - \frac{Ka^2y^2}{2}\right]\mathrm{d}y\right| + C_2 a^{\frac{3}{4}-p_1}.
\end{aligned}$$

Here we use in the first and the second inequality that $\xi^{1-d} < \xi_b^{1-d}$ and $a^{\frac{3}{4}}\xi_b \ll a^{\frac{3}{4}-p_1}$ (since $\xi_b \ll a^{-p_1}$) where $p_1 > 0$ can still be chosen. For the last inequality we use continuous induction on the part in R containing the ϕ-term.

Upon assuming that for every $\xi_b < \xi < \xi_{\max}$

$$\frac{1}{A^2(\xi_b)}\left|\int_{\xi_b}^{\xi} A^2(y)\left[\frac{d-2+2K}{2} - K(b+1)A^2(y) - \frac{Ka^2y^2}{2}\right]\mathrm{d}y\right| \leq ca^{-\frac{3}{4}+l}$$

for some $c > 0$, we do indeed find that

$$|\phi(\xi)| \leq ca^{l_1}$$

where $l_1 = \min(\frac{3}{4} - p_1, l)$. Upon choosing $l > \frac{1}{2}$ and $p_1 = \frac{1}{8}$, the statement of the lemma follows. □

Appendix E. The proof of Lemma 7.2

We use the fact that for $\xi_b < \xi < \xi_{\max}$ the solutions lie at most ca away from the heteroclinic orbit (5.4) of the unperturbed system. As before we denote the second intersection point of the solution with the B-axis by ξ_2. Since we integrate along the heteroclinic orbit, it follows that the integral can only be obtained in one step when $\xi < \xi_2$. In the case where $\xi > \xi_2$, the integral can be bounded by splitting it into two parts, one integrating from ξ_b up to ξ_2 and the other integrating from ξ_2 to ξ. This second part can then be bounded by integrating over one (or more) whole period. Note that this leads to different expressions for the relations between d, K, b and a yielding different c_1, c_2 and c_3 in the statement of the lemma.

Note that $A(\xi_b) < ca^m$ with $\frac{3}{8} < m < 1$, such that integrating from $\xi = 0$ instead of $\xi = \xi_b$ in the integral in (7.1) leads to a difference of at most $ca^{\frac{6}{8}}$. Hence, from now on, we integrate from $\xi = 0$ onwards where we take the error of $ca^{\frac{6}{8}}$ into account. Assuming that $\xi < \xi_2$ and that ξ corresponds to some $y_1 \in (-\infty, \infty)$, we find

$$\begin{aligned}
&\left|\int_{\xi_b}^{\xi} A^2(y)\left[\frac{d-2+2K}{2} - K(b+1)A^2(y) - \frac{K\eta^2}{2}\right]\mathrm{d}y\right| \\
&= \left|\int_{0}^{\xi} A^2(y)\left[\frac{d-2+2K}{2} - K(b+1)A^2(y) - \frac{K\eta^2}{2}\right]\mathrm{d}y + ca^{\frac{6}{8}}\right| \\
&= \left|\int_{-\infty}^{y_1} 2\alpha^2\operatorname{sech}^2(\alpha y)\left[\frac{d-2+2K}{2} - 2K(b+1)\alpha^2\operatorname{sech}^2(\alpha y) - \frac{K\eta^2}{2}\right]\mathrm{d}y + ca^{\frac{3}{4}}\right| \\
&= 2\alpha\left|\left[\left(\frac{d-2}{2} - K + \frac{2}{3}(2b-1)K\alpha^2\right)(\tanh(\alpha y_1)+1) - \frac{2}{3}K(b+1)\alpha^2\frac{\sinh(\alpha y_1)}{\cosh^3(\alpha y_1)}\right] + ca^{\frac{3}{4}}\right| \\
&\leq 4\left|\frac{d-2}{2} - K - \frac{2}{3}K(1-2b)\alpha^2\right| + \frac{4}{27}K(b+1)\sqrt{3}\alpha^2 + ca^{\frac{3}{4}}
\end{aligned}$$

$$= |c_1(d-2) - c_2K + c_3b + ca^{\frac{3}{4}}|. \tag{E.1}$$

In the case where $\xi > \xi_2$, we can bound the integral by adding integrating of the heteroclinic orbit over one or more whole periods to this expression. Hence, we must add

$$\left|\int_{-\infty}^{\infty} 2\alpha^2 \operatorname{sech}^2(\alpha y)\left[\frac{d-2+2K}{2} - 2K(b+1)\alpha^2 \operatorname{sech}^2(\alpha y) - \frac{K\eta^2}{2}\right] \mathrm{d}y\right| = 4\alpha\left|\frac{d-2}{2} - K - \frac{2}{3}K(1-2b)\alpha^2\right| \tag{E.2}$$

or a (positive) integer multiple of this expression. This leads to different constants c_i for solutions with a different number of maxima. For an increase in the number of maxima of the solution by 2, expression (E.2) must be added once to (E.1), yielding different c_i's. Note that the constants c_i can unfortunately not be explicitly determined in general.

In general, the restriction (7.1) leads to

$$|c_1(d-2) - c_2K + c_3b + ca^{\frac{3}{4}}| \leq a^{-\frac{3}{4}+l}A^2(\xi_b).$$

Now, there are two possibilities. Either $A(\xi_b)$ is exponentially small (and so is $A(0)$) or $A(\xi_b) = ca^{m_b}$ for some constants $c, m_b > 0$. Assuming that

$$|c_1(d-2) - c_2K + c_3b| \leq ca^{-\frac{3}{4}+l}\mathrm{e}^{-\frac{\tilde{c}}{a}}$$

gives the existence of all solutions in Theorem 2.1. However, changing the assumption to

$$|c_1(d-2) - c_2K + c_3b| \leq ca^{l_1},$$

where $l_1 = \min\{\frac{3}{4}, -\frac{3}{4} + l + 2m_b\}$ and $A(\xi_b) = c_ba^{m_b}$, also gives the existence of several, but not all, of the solutions given in Theorem 2.1. See Remark 7.1 for details of the solutions that are still found under this assumption.

A further calculation yields that for $b = 0$, the restriction reduces for the $k = 2$ solutions to

$$\left|\frac{d-2}{2} - \frac{5}{3}K\right| + \frac{8\sqrt{2}}{9\sqrt{3}}K \leq ca^{-\frac{3}{4}+l}A^2(\xi_b). \quad \square$$

Appendix F. The proof of Lemma 9.1

From the last equation in system (4.2), we derive an expression for ϕ by first integrating this equation from ξ_b up to some $\xi > \xi_b$, and then finding an integrating factor. This leads to

$$\begin{aligned}\phi(\xi) &= \phi(\xi_b)\exp\left[\int_{\xi_b}^{\xi}\chi(z)\mathrm{d}z\right] \\ &\quad + \frac{a}{1+a^2K^2}\int_{\xi_b}^{\xi}\exp\left[\int_{\xi_b}^{\xi}\chi(z)\mathrm{d}z\right]\left(\frac{d-2}{2} + K\left(1 - \frac{a^2y^2}{2} - (1+b)A^2\right) + a^2K^2\left(yB + \frac{d}{2}\right)\right)\mathrm{d}y,\end{aligned} \tag{F.1}$$

where

$$\chi(z) = \frac{1-d}{z} + \frac{Ka^2z}{1+a^2K^2} - 2B(z).$$

And

$$\exp\left[\int_y^{\xi}\chi(z)\mathrm{d}z\right] = \xi^{1-d}y^{d-1}\exp\left[\frac{Ka^2(\xi^2-y^2)}{2(1+a^2K^2)} - 2\int_y^{\xi}B(z)\mathrm{d}z\right].$$

We only need to prove the estimate in the lemma for $\xi = \xi_{\max}$, and this is the choice that we make from now on.

By using the fact that B lies close to the heteroclinic orbit we can estimate the integral of B in a similar way to in the proof of Lemma 7.1. We find that

$$\frac{1}{8}\log a \leq \int_{\xi_b}^{\xi}B\mathrm{d}z \leq \int_{-\frac{3}{8}T_0^{(k)}}^{0}B_0^{(k)}\mathrm{d}z = -\frac{3}{8}\log a$$

and hence,

$$a^{\frac{3}{4}} \leq \exp\left[-2\int_{\xi_b}^{\xi}B\mathrm{d}z\right] \leq a^{-\frac{1}{4}}.$$

Moreover, for all $\xi_b < y < \xi$,

$$\frac{1}{2}\log a = \int_0^{\frac{1}{2}T_0^{(k)}} B_0^{(k)}\mathrm{d}z \le \int_y^{\xi} B\mathrm{d}z \le \int_{-\frac{1}{2}T_0^{(k)}}^{0} B_0^{(k)}\mathrm{d}z = -\frac{1}{2}\log a$$

leading to

$$a^{-1} \ge \exp\left[-2\int_y^{\xi} B\mathrm{d}z\right] \ge a.$$

We now analyse the first term in (F.1) and show that it is much smaller than the second term. After setting $\xi = \xi_{\max}$ and applying the above estimate, we find that the first term in (F.1) can be estimated as

$$|\phi(\xi_b)|\xi_{\max}^{1-d}\xi_b^{d-1}\exp\left[\frac{Ka^2(\xi_{\max}^2-\xi_b^2)}{2(1+a^2K^2)} - 2\int_{\xi_b}^{\xi_{\max}} B\mathrm{d}z\right] \le ca^{p+d-1-\frac{1}{4}}\xi_b^{d-1} \ll ca^{p+d-\frac{5}{4}-\tilde{p}} < ca^{\frac{6}{4}},$$

using that $|\phi(\xi_b)| < Ca^p$ for $p < 1$ (Lemma 4.3) and that $\xi_b \ll ca^{-\tilde{p}}$ for some $\tilde{p} > 0$.

Now we focus on the second term in expression (F.1). We can bound this integral by using that $|B| < 1$ leading to $|a^2K^2(yB + \frac{1}{2})| \le ca^2y \le ca$ and hence the other terms in the integral are dominant compared to this one. Also, using $\exp[\frac{Ka^2(\xi^2-y^2)}{2(1+\varepsilon^2)}] \ge 1$ for every $\xi_b < y < \xi$, and the bound on the integral of B, we find that the second term in (F.1) can (for $\xi = \xi_{\max}$) be bounded from below by

$$\begin{aligned} &a^2\left|\int_{\xi_b}^{\xi_{\max}} \xi_{\max}^{1-d}y^{d-1}\left[\frac{d-2}{2} + K\left(1 - \frac{a^2y^2}{2} - (1+b)A^2\right)\right]\right|\mathrm{d}y \\ &= \left|\frac{a^2\xi_{\max}^{1-d}}{d}\left(\frac{d-2}{2}+K\right)(\xi_{\max}^d - \xi_b^d) - a^4\frac{K}{2(d+2)}\xi_{\max}^{1-d}(\xi_{\max}^{d+2} - \xi_b^{d+2}) - a^2K(1+b)\xi_{\max}^{1-d}\int_{\xi_b}^{\xi_{\max}} y^{d-1}A^2\mathrm{d}y\right| \\ &= \left|\frac{a(d-2)}{d}\left(1 - \frac{2K}{d+2}\right) - a^2K(1+b)\xi_{\max}^{1-d}\int_{\xi_b}^{\xi_{\max}} y^{d-1}A^2\mathrm{d}y\right|. \end{aligned}$$

Next, we show that the latter term in this expression is much smaller than the first.

The integral of A^2 can be estimated by using the fact that A lies close to the heteroclinic orbit; hence

$$\begin{aligned} \xi_{\max}^{1-d}\int_{\xi_b}^{\xi_{\max}} y^{d-1}A^2\mathrm{d}y &\le \tilde{m}\int_{-\infty}^{\infty} 2\alpha^2\,\mathrm{sech}^2(\alpha z)\mathrm{d}z \\ &= 2\tilde{m}\,[\tanh(\alpha z)]_{-\infty}^{\infty} = 4\tilde{m}\alpha \le 4\tilde{m}, \end{aligned}$$

where $\tilde{m}$ is a positive integer denoting the number of round-trips that the solution makes through the (A, B)-plane.

We conclude that the second term in (F.1) is larger than Ca for some positive constant C, and hence, it is much larger than the first term in (F.1). Moreover,

$$|\phi(\xi_{\max})| \ge Ca \gg ca^{d-\frac{1}{2}},$$

concluding the statement in the lemma.

Appendix G. The proof of Lemma 9.2

We will bound the terms in $\frac{\partial\psi_d^0(\xi)}{\partial\Delta}$ separately. An estimate for the first term in $\frac{\partial\psi_d^0(\xi)}{\partial\Delta}$ follows from using the result in Lemma 4.3 where we showed that

$$|I(\xi)| \le CA^2(\xi)\xi^d$$

for $\xi \le \xi_b$.

Also, the term $\frac{1}{A}\frac{\mathrm{d}A}{\mathrm{d}\Delta}$ appears in the expression for $\frac{\partial\psi_d^0(\xi)}{\partial\Delta}$, and therefore, we must study it. We will show in Appendix I that $\frac{1}{A}\frac{\mathrm{d}A}{\mathrm{d}\Delta} \le \hat{c}\log(\xi)$ as long as $\xi \le \xi_b$.

Hence,

$$\begin{aligned} \left|\frac{a\xi^{1-d}I(\xi)}{A^2(\xi)(1+a^2K^2)}\left(\log\xi + \frac{2}{A(\xi)}\frac{\mathrm{d}A}{\mathrm{d}\Delta}\right)\right| &\le C\frac{a\xi^{1-d}|I(\xi)|}{A^2(\xi)}\log\xi \\ &\le ca\xi\log\xi \ll ca^{\frac{3}{4}}, \end{aligned}$$

for every $\xi \leq \xi_b$.

Moreover,

$$\left| \int_0^\xi A^2 y^{d-1} R(y) \frac{2}{A} \frac{\mathrm{d}A}{\mathrm{d}\Delta} \mathrm{d}y \right| \leq 2 \int_0^\xi A^2 y^{d-1} |R(y) \log y| \mathrm{d}y.$$

Using this bound, and then splitting the integral I_1 into two parts we find that

$$\begin{aligned}
|I_1| &\leq c \int_0^\xi A^2 y^{d-1} |R(y) \log y| \mathrm{d}y \\
&= c \int_0^1 A^2 y^{d-1} |R(y) \log y| \mathrm{d}y + c \int_1^\xi A^2 y^{d-1} |R(y) \log y| \mathrm{d}y \\
&\leq -C A^2(\xi) \int_0^1 y^{d-1} \log y \mathrm{d}y + c \log \xi \int_1^\xi A^2 y^{d-1} |R(y)| \mathrm{d}y \\
&\leq -C A^2(\xi) \left[\frac{1}{d} y^d \log y - \frac{1}{d^2} y^d \right]_0^1 + \log \xi C_1 A^2(\xi) \xi^d \\
&= c A^2(\xi)(1 + c_1 \xi^d \log \xi),
\end{aligned}$$

where we use that $|R(y)| \leq C$ for $0 < y < 1$ and that $\log y \leq \log \xi$ for $1 < y < \xi$. Concluding, we find that

$$\frac{a \xi^{1-d} |I_1|}{A^2(\xi)(1 + a^2 K^2)} \leq c a \xi^{1-d} (1 + c_1 \xi^d \log \xi) \ll c a^{\frac{3}{4}},$$

for every $\xi \leq \xi_b$.

To obtain a bound for I_2, we use continuous induction to handle the part which contains $\frac{\partial \phi(\xi)}{\partial \Delta}$. First, we study the function S. By using that for every $\xi \leq \xi_b$, $|A \frac{\mathrm{d}A}{\mathrm{d}\Delta}| \leq c A^2 \log y \leq c a^{2m} \log y \ll c a^m$, $|\frac{\partial \psi(\xi)}{\partial \Delta}| \leq c a^{\frac{3}{4}}$, and $|\phi| < c a^p$ we find that

$$(d-2) S(y) = R(y),$$

to leading order. Hence, it follows that

$$|I_2| \leq |I|.$$

Combining the above results we find that

$$\left| \frac{\partial \psi_d^0(\xi)}{\partial \Delta} \right| \ll c a^{\frac{3}{4}},$$

for every $\xi \leq \xi_b$. □

Appendix H. The proof of Lemma 9.3

In this proof we use the expression for ψ that we obtained in the proof of Lemma 9.1. Differentiating (F.1) with respect to Δ we obtain

$$\begin{aligned}
\frac{\partial \psi(\xi)}{\partial \Delta} &= \frac{\partial \psi(\xi_b)}{\partial \Delta} \exp\left[\int_{\xi_b}^\xi \chi(z) \mathrm{d}z \right] + \phi(\xi_b) \exp\left[\int_{\xi_b}^\xi \chi(z) \mathrm{d}z \right] \left[\log \xi^{-1} + \log \xi_b + \frac{k_1 a^2}{1 + a^2 K^2} (\xi^2 - \xi_b^2) - 2 \int_{\xi_b}^\xi \frac{\partial B}{\partial \Delta} \mathrm{d}z \right] \\
&\quad + \frac{a}{1 + a^2 K^2} \int_{\xi_b}^\xi \exp\left[\int_y^\xi \chi(z) \mathrm{d}z \right] \left[\left(\log \xi^{-1} + \log y + \frac{k_1 a^2}{1 + a^2 K^2} (\xi^2 - y^2) \right. \right. \\
&\quad \left. - 2 \int_y^\xi \frac{\partial B}{\partial \Delta} \mathrm{d}z \right) \left(\frac{d-2}{2} + K \left(1 - \frac{a^2 y^2}{2} - (1+b) A^2 \right) + a^2 K^2 \left(y B + \frac{d}{2} \right) \right) + \frac{1}{2} \\
&\quad \left. + k_1 \left(1 - \frac{a^2 y^2}{2} - (1+b) A^2 \right) - 2K(1+b) A \frac{\partial A}{\partial \Delta} + 2K k_1 a^2 \left(y B + \frac{d}{2} \right) + K^2 a^2 \left(y \frac{\partial B}{\partial \Delta} + \frac{1}{2} \right) \right] \mathrm{d}y \\
&= T_1 + T_2 + T_3,
\end{aligned}$$

where χ is given in Appendix F.

We only need to bound $\frac{\partial \psi}{\partial \Delta}$ at $\xi = \xi_{\max}$ and this is the choice that we make from now on. In the following, we show that at $\xi = \xi_{\max}$, T_3 is dominant with respect to the other two terms. Using the estimate for $\exp[-2 \int_{\xi_b}^\xi B(z) \mathrm{d}z]$ obtained in the proof of

Lemma 9.1, we find that $\exp[\int_{\xi_b}^{\xi_{\max}} \chi(z)\mathrm{d}z] \leq ca^{d-\frac{5}{4}-\tilde{p}}$ for some $\tilde{p} > 0$. Combining this with the fact that $|\frac{\partial\psi(\xi_b)}{\partial\Delta}| \leq ca^{\frac{3}{4}}$ as given in Lemma 9.2 we get that

$$|T_1| \leq ca^{d-\frac{5}{4}-\tilde{p}+\frac{3}{4}} = ca^{d-\frac{3}{4}} \ll ca,$$

at $\xi = \xi_{\max}$, since $d > 2$. In the above we can still choose $\tilde{p}$ as long as it is positive; therefore, we take $\tilde{p} = \frac{1}{4}$.

We showed in Lemma 7.1 that $|\phi| < ca^{\frac{1}{2}}$, and hence,

$$\left|\phi(\xi_b)\exp\left[\int_{\xi_b}^{\xi}\chi(z)\mathrm{d}z\right]\right| \ll ca^{d-\frac{3}{4}-p}$$

where $p > 0$ can still be chosen. Also, in Appendix I we show that $\frac{\mathrm{d}B}{\mathrm{d}\Delta} = \mathcal{O}(a)$ for $\xi_b < \xi < \xi_{\max}$; hence,

$$\int_{\xi_b}^{\xi}\frac{\partial B}{\partial\Delta}\mathrm{d}y \leq ca\xi \leq ca\xi_{\max} = C_1.$$

Therefore, at $\xi = \xi_{\max}$,

$$|T_2| \leq ca^{d-\frac{3}{4}-p}\left[\log\xi_{\max} + \log\xi_b + C\right] \ll c_1a^{d-\frac{3}{4}-\frac{1}{16}} < c_1a^{\frac{19}{16}} \ll c_1a$$

using that $\log\xi_{\max} \ll a^{-p_1}$ for some $p_1 > 0$, and choosing $p_1 + p = \frac{1}{16}$.

Now, we bound T_3 by applying that $\log y \gg a^2y^2$ and $\log y \gg ay$ for every $y \geq \xi_b \gg 1$. Also, we use $|B| < 1$, $A\frac{\mathrm{d}A}{\mathrm{d}\Delta} = \mathcal{O}(a)$ and $\frac{\mathrm{d}B}{\mathrm{d}\Delta} = \mathcal{O}(a)$ for $\xi_b < \xi < \xi_{\max}$, which gives that to leading order

$$\begin{aligned}T_3 &= a\int_{\xi_b}^{\xi}\exp\left[\int_y^{\xi}\chi(z)\mathrm{d}z\right]\left[\left(\log\xi^{-1}+\log y\right)\left(\frac{d-2}{2}+K\left(1-\frac{a^2y^2}{2}-(1+b)A^2\right)\right)+\frac{1}{2}\right.\\ &\quad\left.+\,k\left(1-\frac{a^2y^2}{2}-(1+b)A^2\right)\right]\mathrm{d}y\\ &= a\int_{\xi_b}^{\xi}\exp\left[\int_y^{\xi}\chi(z)\mathrm{d}z\right]\left(\log\xi^{-1}+\log y+\frac{1}{d-2}\right)\left(\frac{d-2}{2}+K\left(1-\frac{a^2y^2}{2}-(1+b)A^2\right)\right)\mathrm{d}y.\end{aligned}$$

In the proof of Lemma 9.1 we obtained that $\exp[-2\int_y^{\xi}B] \geq ca$; thus,

$$|T_3| \geq a^2\int_{\xi_b}^{\xi}\xi^{1-d}y^{d-1}\left|\left(\log\xi^{-1}+\log y+\frac{1}{d-2}\right)\left(\frac{d-2}{2}+K\left(1-\frac{a^2y^2}{2}-(1+b)A^2\right)\right)\right|\mathrm{d}y.$$

Integrating and substituting $\xi = \xi_{\max}$ yields to leading order

$$\begin{aligned}&a^2\int_{\xi_b}^{\xi_{\max}}\xi_{\max}^{1-d}y^{d-1}\left(\log\xi_{\max}-\log y-\frac{1}{d-2}\right)\left(\frac{d-2}{2}+K\left(1-\frac{a^2y^2}{2}\right)\right)\mathrm{d}y\\ &\quad=\frac{2a}{d^2(d+2)^2}\left|-(d+2)^2+2K(3d+2)\right| = Ca,\end{aligned}$$

where $C > 0$.

Moreover,

$$\begin{aligned}a^2\int_{\xi_b}^{\xi_{\max}}\xi_{\max}^{1-d}y^{d-1}\left(\log\xi_{\max}-\log y-\frac{1}{d-2}\right)(1+b)A^2\mathrm{d}y &\leq \hat{C}a^2\log\xi_{\max}\int_{\xi_b}^{\xi_{\max}}A^2\mathrm{d}y\\ &\leq C_1a^2\log\xi_{\max} \leq C_1a^{\frac{3}{2}}\end{aligned}$$

using the estimate for the integral of A^2 obtained in the proof of Lemma 9.1.

Combining these bounds finally gives

$$|T_3| \geq Ca.$$

Hence, the terms T_1 and T_2 are much smaller than T_3 for $\xi = \xi_{\max}$, and

$$\left|\frac{\partial\psi_d^0(\xi_{\max})}{\partial\Delta}\right| \geq Ca > c_1a^{d-\frac{1}{2}},$$

since $d > \frac{3}{2}$. □

Appendix I. Bounds for $\frac{\mathrm{d}A}{\mathrm{d}\Delta}$ and $\frac{\mathrm{d}B}{\mathrm{d}\Delta}$

In this appendix, we derive the bounds on $\frac{\mathrm{d}A}{\mathrm{d}\Delta}$ and $\frac{\mathrm{d}B}{\mathrm{d}\Delta}$ as used in the proofs of Lemmas 9.2 and 9.3.

For $\xi \leq \xi_b$ we obtain an estimate for $\frac{\mathrm{d}A}{\mathrm{d}\Delta}$ by using that A lies $\mathcal{O}(a)$ close to the solutions R of (4.1). We know from the proof of Lemma 4.1 that for $\xi \gg 1$, $A = \xi^{\frac{1-d}{2}}\left[a_1 \mathrm{e}^{-\xi} + b_1 \mathrm{e}^{\xi}\right]$ to leading order. Moreover, $A \leq ca^m$ for $\xi \leq \xi_b$; hence, as long as $\xi \leq \xi_b$,

$$\frac{\mathrm{d}A}{\mathrm{d}\Delta} = cA(\xi)\log\xi.$$

To determine an estimate on $\frac{\mathrm{d}A}{\mathrm{d}\Delta}$ and $\frac{\mathrm{d}B}{\mathrm{d}\Delta}$ for $\xi_b \leq \xi \leq \xi_{\max}$, we use the fact that the constructed solution lies $\mathcal{O}(a)$ close to the heteroclinic orbit of the unperturbed system, (2.12) with $a = 0$. Thus, $A(\xi) = A^{(k)}(\xi) + \mathcal{O}(a)$ and $B(\xi) = B^{(k)}(\xi) + \mathcal{O}(a)$ for $\xi_b \leq \xi \leq \xi_{\max}$, where $k \to 1$. Here, $A^{(k)}(\xi)$ and $B^{(k)}(\xi)$ do not depend on the dimension d. Hence, $\frac{\mathrm{d}A}{\mathrm{d}\Delta} = \mathcal{O}(a)$ and $\frac{\mathrm{d}B}{\mathrm{d}\Delta} = \mathcal{O}(a)$ for $\xi_b \leq \xi \leq \xi_{\max}$. □

References

[1] M. Abramovitz, I.A. Stegun, Handbook of Mathematical Functions with Formulas, Graphs and Mathematical Tables, Dover, New York, 1972.
[2] I.S. Aranson, L. Kramer, The world of the complex Ginzburg–Landau equation, Rev. Modern Phys. 74 (2002) 99–143.
[3] H.R. Brand, P.S. Lomdahl, A.C. Newell, Benjamir–Feir turbulence in convective binary fluid mixtures, Physica D 23 (1986) 345–362.
[4] C.J. Budd, Asymptotics of multi-bump blow-up self-similar solutions of the nonlinear Schrödinger equation, SIAM J. Appl. Math. 62 (3) (2002) 801–830.
[5] C.J. Budd, S. Chen, R.D. Russell, New self-similar solutions of the nonlinear Schrödinger equation with moving mesh computations, J. Comput. Phys. 152 (1999) 756–789.
[6] C.J. Budd, V. Rottschäfer, J.F. Williams, Multi-bump, blow-up, self-similar solutions of the complex Ginzburg–Landau equation, SIAM J. Appl. Dyn. Syst. 4 (3) (2005) 649–678.
[7] P.F. Byrd, M.D. Friedman, Handbook of Elliptic Integrals for Engineers and Physicists, Springer-Verlag, Berlin, Göttingen, Heidelberg, 1954.
[8] A. Davey, L.M. Hocking, K. Stewartson, On the nonlinear evolution of three-dimensional disturbances in plane Poiseuille flow, J. Fluid Mech. 63 (1974) 529–536.
[9] R.C. DiPrima, H.L. Swinney, Instabilities and transition in flow between concentric cylinders, in: H. Swinney, J. Gollub (Eds.), Hydrodynamic Instabilities and the Transition to Turbulence, in: Topics in Applied Physics, vol. 45, Springer-Verlag, New York, 1981.
[10] N. Fenichel, Geometric singular perturbation theory for ordinary differential equations, J. Differential Equations 31 (1979) 53–98.
[11] J. Guckenheimer, P.J. Holmes, Nonlinear Oscillations, Dynamical Systems, and Bifurcations of Vector Fields, in: Applied Mathematical Sciences Series, vol. 42, Springer-Verlag, New York, 1983.
[12] C.K.R.T. Jones, Geometric singular perturbation theory, in: Dynamical Systems, Montecatini Terme, in: R. Johnson (Ed.), Lect. Notes Math., vol. 1609, Springer-Verlag, New York, 1994, pp. 44–118.
[13] C.K.R.T. Jones, T.J. Kaper, N. Kopell, Tracking invariant manifolds up to exponentially small errors, SIAM J. Math. Anal. 27 (1996) 558–577.
[14] T.J. Kaper, C.K.R.T. Jones, A primer on the exchange lemma for fast–slow systems, in: Multiple-Time-Scale Dynamical Systems, in: C.K.R.T. Jones, A. Khibnik (Eds.), IMA Volumes on Mathematics and its Applications, vol. 122, Springer, New York, 2001, pp. 65–88.
[15] N. Kopell, M. Landman, Spatial structure of focusing singularity of the nonlinear Schrödinger equation: A geometrical analysis, SIAM J. Appl. Math. 55 (1995) 1297–1323.
[16] A. Mielke, The Ginzburg–Landau Equation in its Role as a Modulation Equation, in: Handbook of Dynamical Systems, vol. 2, North-Holland, 2002, pp. 759–834.
[17] A.I. Neihstadt, Passage through a separatrix in a resonance problem with a slowly varying parameter, PMM 39 (1975) 594–605.
[18] A.C. Newell, J.A. Whitehead, Finite bandwidth, finite amplitude convection, J. Fluid Mech. 28 (1969) 279–303.
[19] P. Plecháč, V. Šverák, On self-similar singular solutions of the complex Ginzburg–Landau equation, Comm. Pure Appl. Math. 54 (2001) 1215–1242.
[20] V. Rottschäfer, T. Kaper, Blowup in the nonlinear Schrödinger equation near critical dimension, JMAA 268 (2) (2002) 517–549.
[21] V. Rottschäfer, T. Kaper, Geometric theory for multi-bump, self-similar, blowup solutions of the cubic nonlinear Schrödinger equation, Nonlinearity 16 (3) (2003) 929–961.
[22] C. Robinson, Sustained resonance for a nonlinear system with slowly varying coefficients, SIAM J. Math. Anal. 14 (1983) 847–960.
[23] K. Stewartson, J. Stuart, A nonlinear instability theory for a wave system in plane Poiseuille flow, J. Fluid Mech. 48 (1971) 529–545.
[24] C. Sulem, P.L. Sulem, The Nonlinear Schrödinger Equation: Self-focusing and Wave Collapse, in: Applied Mathematical Sciences Series, vol. 139, Springer, New York, 1999.